



**SIMULATIONS OF FLOWING  
SUPERCRITICAL N-DECANE**

THESIS

Jeffery T. Thornburg, Lieutenant, USAF

AFIT/GAE/ENY/00M-12

20000803 143

**DEPARTMENT OF THE AIR FORCE  
AIR UNIVERSITY**

**AIR FORCE INSTITUTE OF TECHNOLOGY**

---

---

**Wright-Patterson Air Force Base, Ohio**

APPROVED FOR PUBLIC RELEASE; DISTRIBUTION UNLIMITED.

DTIC QUALITY INSPECTED 4

### **Disclaimer**

The views expressed in this thesis are those of the author and do not reflect the official policy or position of the United States Air Force, the Department of Defense, or the United States Government.

AFIT/GAE/ENY/00M-12

SIMULATIONS OF FLOWING SUPERCRITICAL N-DECANE

THESIS

Presented to the Faculty

Department of Aeronautics and Astronautics

Graduate School of Engineering and Management

Air Force Institute of Technology

Air University

Air Education and Training Command

In Partial Fulfillment of the Requirements for the

Degree of Master of Science in Aeronautical Engineering

Jeffery T. Thornburg, B.S.

Lieutenant, USAF

March 2000


Approved for public release; distribution unlimited

AFIT/GAE/ENY/00M-12

SIMULATIONS OF FLOWING SUPERCRITICAL N-DECANE

Jeffery T. Thornburg  
First Lieutenant, USAF

Approved:



Lt. Col. Jeffery Little  
Committee Chairman

28 Feb 2000

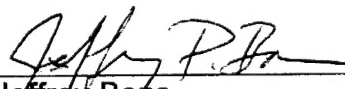
Date



Dr. Milt Franke  
Committee Member

28 Feb 2000

Date



Major Jeffrey Bons  
Committee Member

28 Feb 2000

Date

## **Acknowledgments**

I would like to thank everyone who helped me immensely throughout this study. Without the kind and expeditious assistance of Dr. Jamie Ervin, this study would not have been possible. I would also like to thank Rich Striebich and Dennis for all their time and help with the STDS. Under a busy schedule, Rich always found time to help me understand and operate his "baby". Also, I was given a lot of generous latitude in this study due to the efforts and understanding of my advisor, Lieutenant Colonel Jeff Little. I would like to thank him for letting me find my own way and for truly teaching me what it is to become an engineer. Finally, I would like to thank my beautiful wife, Jody, for all her love and support, for indulging me in all those weekend homework marathons, and all that time I spent behind the computer. I promise to make it up in the coming year.

Jeff Thornburg

## Table of Contents

	Page
Acknowledgments .....	iv
Table of Contents .....	v
List of Figures .....	vii
List of Tables .....	ix
List of Notation .....	x
Abstract .....	xi
I. Introduction and Objectives .....	1
Introduction .....	1
Objectives .....	2
II. Literature Review .....	3
Supercritical Fluids .....	3
Thermal Oxidation Research .....	4
Pyrolytic Research .....	9
III. Experimental Setup and Procedure .....	11
IV. Computational Model of the Reactor .....	18
Radiation Effects .....	25
STDS Temperature Profiles .....	27
V. Results and Discussion .....	29
STDS Reactor Simulations .....	29
Larger Reactor Simulation .....	36
VI. Summary, Conclusions, and Recommended Future Work .....	39

Summary and Conclusions .....	39
Recommended Future Work.....	40
VII. Bibliography .....	42
Appendix A.....	45
Sample Input File for STDS Reactor Simulations .....	45
Appendix B.....	48
Sample Input File for Goel's Reactor Simulations.....	48
Appendix C.....	51
Finite Difference Analysis to Study Inner and Outer Reactor Wall.....	51
Assuming 200°C Fluid Temperature at Reactor Entrance .....	53
Appendix D.....	55
Graphical Representations of Radiation Study Temperature Profiles .....	55
Vita .....	57

## List of Figures

	Page
Figure 1: Phase Diagram Showing Supercritical Region.....	4
Figure 2: Predicted and measured dissolved O <sub>2</sub> (16mL/min and Jet A) [5] .....	8
Figure 3: Sample Introduction System for CPTC [2] .....	14
Figure 4: Photo of Sparger, Pump, and Dampener Assembly.....	15
Figure 5: Photo of Flowing Switch Valve Assembly .....	15
Figure 6: Thermal Reaction Compartment for CPTC [2] .....	16
Figure 7: Photo of Thermal Reaction Compartment.....	17
Figure 8: Photo of 30 cm Reactor Coil Inside High Temp Furnace .....	18
Figure 9: Schematic Representation of CFD-ACE™ [22] .....	19
Figure 10: Solution Flowchart for SIMPLEC Algorithm [22].....	21
Figure 11: High Temperature Reactor Grid (Axisymmetric) .....	24
Figure 12: Decane Decomposition at 0.5 mL/min.....	30
Figure 13: Decane Decomposition at 0.7 mL/min.....	30
Figure 14: Wall and Bulk Temperature Profile for Reactor at 0.5 mL/min and 390°C .....	33
Figure 15: Wall and Bulk Temperature Profile for Reactor at 0.5 mL/min and 550°C .....	33
Figure 16: Wall and Bulk Temperature Profile for Reactor at 0.5 mL/min and 630°C .....	34
Figure 17: Wall and Bulk Temperature Profile for Reactor at 0.7 mL/min and 390°C .....	34



Figure 18: Wall and Bulk Temperature Profile for Reactor at 0.7 mL/min and 550°C .....	35
Figure 19: Wall and Bulk Temperature Profile for Reactor at 0.7 mL/min and 630°C .....	35
Figure 20: Comparison of Goel's Dodecane Data and Decane CFDC Model ....	39

## List of Tables

	Page
Table 1: Differences in Transport Properties Between Liquids, Gases, and Supercritical Fluids .....	4
Table 2: Temperature Data for Argon Flow Through Reactor .....	25
Table 3: Temperature Data for Argon Flow with Circulation Air .....	26
Table 4: Temperature Data for Decane Flow at 0.5 mL/min and 750 psi .....	27
Table 5: Temperature Data for Decane Flow at 0.5 mL/min and 750 psi .....	28
Table 6: Temperature Data for Decane Flow at 0.7 mL/min and 750 psi .....	28
Table 7: Temperature Data for Decane Flow at 0.7 mL/min and 750 psi .....	28
Table 8: Summary of Parameters for High Temperature Flow Reactor .....	32
Table 9: Summary of Parameters for Goel's Dodecane Flow Reactor .....	37

## List of Notation

STDS - System for Thermal Diagnostic Studies

CFDC - Computational Fluid Dynamics with Chemistry

$A_0$  - Pre-Exponential Factor for Arrhenius Equation (1/seconds)

$E_a$  - Activation Energy for Chemical Reaction (kcal/gram-mole)

SUPERTRAPP - NIST Mixture Database for Thermophysical Properties

Re - Reynolds Number

Decane -  $C_{10}H_{22}$

Dodecane -  $C_{12}H_{26}$

GC - Gas Chromatography

MS - Mass Spectrometry

GUI - Graphical User Interface

### **Abstract**

The Air Force is interested in the research of supercritical jet and rocket fuels, as well as the effects of thermally induced fuel degradation. As future flight vehicles travel at ever increasing Mach numbers, greater heat loads will be imposed upon the fuel.

The primary purpose of this study is to develop a computational model for predicting fuel decomposition and bulk fuel temperatures in a simulated heated flow reactor. The System for Thermal Diagnostic Studies (STDS), located in the Air Force Research Laboratory's Fuels Branch, is used to analyze fuels under supercritical temperatures and pressures. Computational simulations of the STDS reactor are performed to better understand the heat transfer, fluid dynamics, and chemistry associated with fuel flow through the STDS reactor. A simplified global chemistry model is incorporated into the computational simulation.

Predictions of the current model are compared to the results of the STDS experiments, which employ flowing n-decane. The proposed computational model is validated using experimental data obtained at different flow rates after thermally stressing the n-decane fuel. The model predictions agree well with the experimentally measured results. The computational model serves as a tool to study how various physical and experimental parameters affect fuel degradation.

# SIMULATIONS OF FLOWING SUPERCRITICAL N-DECANE

## I. Introduction and Objectives

### Introduction

There is increased interest to develop advanced jet and rocket fuels for future aircraft and spacecraft designs. Aircraft use jet fuel to cool engine oils, hydraulic fluids, avionics, and electrical systems. As future flight vehicles travel at ever increasing Mach numbers, greater heat loads will be imposed upon the fuel. These heat loads will manifest themselves in higher fuel temperatures, and unfortunately, degradation of the fuel.

Advanced computational fluid dynamic models with fuel degradation chemistry are needed to determine the impact of fuel degradation in these advanced flight vehicles. A realistic model can assist in the identification of complex processes, which occur in the fuel flow system under varying conditions. Currently, it is impractical to build a comprehensive model of real jet and rocket fuel decomposition in a flight vehicle because of the many physical and chemical processes that are not well understood. So this study focuses on an accurate description of the fluid dynamics, with a simplified global chemistry model to examine the fuel degradation in a reactor tube.

For a better understanding of fuel degradation, it is important to note that fuel thermal decomposition occurs by means of two processes, thermal oxidation and pyrolysis. Thermal oxidation occurs when the fuel reacts with oxygen that is dissolved in the fuel; this begins around 100°C for conventional fuels. The

oxygen is completely consumed at temperatures above 315°C, but can be completely consumed at lower temperatures. Pyrolysis occurs in fuels when the temperature is above 480°C. The fuel thermally cracks and pyrolytic deposits become a problem at these temperatures. This study was conducted where temperatures are above 480°C and pyrolysis is dominant. The numerical model constructed uses the computational fluid dynamics code CFD-ACE™ with a global chemical kinetic model for flowing n-decane.

## **Objectives**

Despite the complexity of developing a comprehensive model to study fuel decomposition in reactor or other flow, a simplified model can yield valuable insight into the problem. The primary purpose of this research is to develop a practical computational model for predicting fuel decomposition and bulk fuel temperatures in a simulated heated flow reactor for specific boundary conditions and parameters.

This model is required to simulate a system of fluid dynamics coupled with chemical reactions and heat transfer. This system is solved with the commercial code CFD-ACE™. The System for Thermal Diagnostic Studies (STDS) serves as the experimental platform for the computational model. The geometry and flow conditions of the STDS with n-decane fuel were simulated, and those results were validated with the experimental data from the STDS. The intent is for this

computational model to provide a better understanding of flow reactor experiments with fuel decomposition.

## **II. Literature Review**

In order to begin a discussion of the present reactor flow, it is important to understand the characteristics of supercritical fluids. Fluid properties in the supercritical regime must be understood in order to develop a reasonable computational model for the reactor operating at supercritical conditions.

### **Supercritical Fluids**

A supercritical fluid is defined as a substance that is above its critical temperature ( $T_c$ ) and critical pressure ( $P_c$ ) [1]. Figure 1 shows the supercritical region in a phase diagram. Supercritical fluids exhibit physical and chemical properties intermediate between those of liquids and gases. Mass transfer is rapid with supercritical fluids, and their dynamic viscosities are similar to those found in normal gaseous states. The diffusivity of the supercritical fluid is much greater than that of a liquid. Table 1 displays differences in transport properties between supercritical fluids, gases, and liquids [2]. As, shown, changes in viscosity and diffusivity are more pronounced in the region of the critical point. Even at high pressures (300-400 atm) viscosity and diffusivity are 1-2 orders of magnitude different from liquids.

**Table 1: Differences in Transport Properties Between Liquids, Gases, and Supercritical Fluids [2]**

	<i>Liquid</i>	<i>Supercritical Fluid</i>	<i>Gas</i>
Solvation (solute(g)/solvent(g))	1.0	0.1	$\approx 0$
Density (e.g., dodecane, g/ml)	0.75 (25°C)	$\approx 0.2$	P,T dependent
Diffusivity (cm <sup>2</sup> /sec)	$10^{-5}$	$10^{-3}$	$10^{-1}$
Viscosity	$10^{-2}$	$10^{-3}$	$10^{-4}$

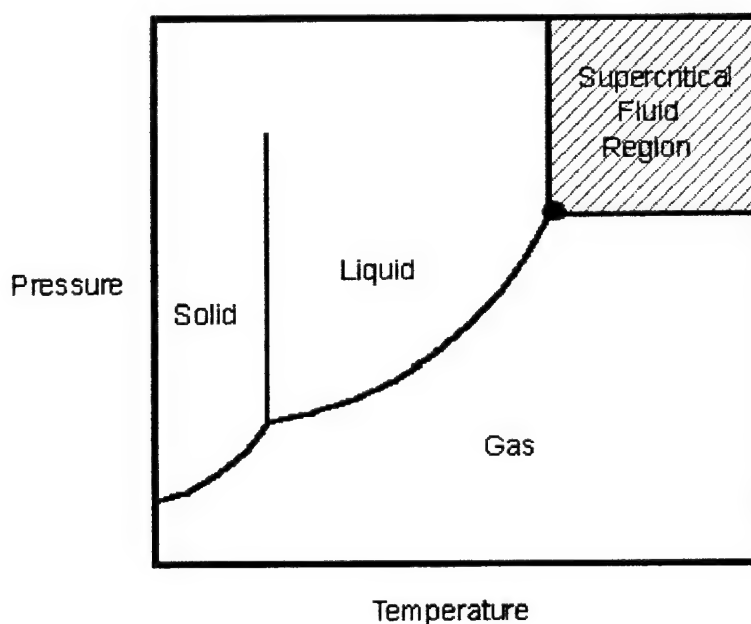


**Figure 1: Phase Diagram Showing Supercritical Region**

## Thermal Oxidation Research

Early thermal oxidative work was primarily focused below the supercritical regime. For example, the critical temperature and pressure of n-decane is 344°C and 20.8 atmospheres respectively. Numerous experiments have been conducted which varied residence time, temperature, and reactive atmosphere,



while measuring product and deposit formation. This experimental research was also accompanied by attempts to model the results with increasingly complex chemical analysis. A large amount of experimental data has been generated in the area of thermal degradation of jet fuels. Unfortunately, the exact detailed mechanisms that govern thermal oxidation and pyrolysis are unknown. Global chemistry models have been used to correlate data from various experiments to improve understanding of the fuel degradation phenomenon.

Taylor [3] used a heated 304 stainless steel tube to transport JP-5 and various jet fuels into a four-zone high temperature furnace at pressures up to 1,000 psi and maximum temperatures near 649°C. Taylor's work primarily focused on the thermal oxidation of jet fuels. His reactor had an average residence time of 25 seconds. Taylor found that deposition with air saturated fuels increased with temperature, then dropped sharply in a transition zone between 350°C and 425°C, where the dissolved oxygen was consumed [3]. It was found that the reduction of oxygen within the fuel would reduce the rate of deposits. The pressure in the experiments was varied from 18 to 69 atm to study its effect. Taylor found the effect of pressure to be a complex one, particularly when pressure is varied below and above the critical pressure, where supercritical properties of the fuel influence the deposition process. This is of particular interest in the current study, because the pressure will be above the critical pressure. Taylor's four temperature zones along the reactor are difficult to understand because of the complex heat transfer and fluid dynamics.

In an effort to obtain a better understanding of the complex chemistry involved with reactor flow, research emerged in the 1990's showcasing computational fluid dynamics with chemistry (CFDC) models of jet fuel degradation. In 1989, Roquemore [10] developed an initial CFDC one step global chemistry model that was later incorporated into a model developed by Krazinski. Krazinski et al. [4] developed a second generation CFDC thermal decomposition model using JP-5 as the fuel. This model showed promising trends that matched experimental data considering it was only a three-step global chemistry model. The model was shown to characterize the trends in fuel deposition rates and demonstrated the coupling between chemistry, fluid dynamics, and heat transfer processes that occur during fuel decomposition. The impact of wall deposits on the heat transfer and fluid dynamics of the system was not incorporated into the model. Krazinski believed that more experiments were needed to validate his model.

Ervin et al. [5] worked on a CFDC model that focused on the cooled regions of a flowing system and how deposition was affected using JP-8 fuel. This model was successful in predicting surface deposition rates for near-isothermal and non-isothermal reactor flows, but was only tested for a temperature range from 25°C to 270°C. Ervin's work utilized additional reaction steps for his global model, but this model was not tested at temperatures leading to pyrolysis, nor did it include conditions in the supercritical regime.

J.S. Ervin and S. Zabarnick [6] created the first CFDC model of jet fuel degradation using pseudo-detailed chemistry. The model is pseudo-detailed

meaning that the chemical kinetics of oxygen consumption are described using several reactions representing the dominant chemistry rather than using hundreds of reactions found in a detailed model. Pseudo-detailed kinetic modeling relies on rate parameters that are more realistic than simpler global kinetic parameters [6]. With this pseudo-detailed approach, dissolved oxygen measurements are used to characterize fuels over wide temperature ranges, and no assumption of the value of the overall reaction order needs to be made. This modeling is believed to offer promise in extending simulation capabilities to include the effects of fuel additives. Ervin and Zabarnick used a heat exchanger, which simulated a complex thermal flow environment. Oxygen consumption and production of hydroperoxides were measured for both Jet A and Jet A-1 fuel. The model performed well in matching the experimental data as seen in Figure 2; however, this study did not include pyrolytic temperatures or supercritical conditions as its primary purpose was to study thermal oxidation.

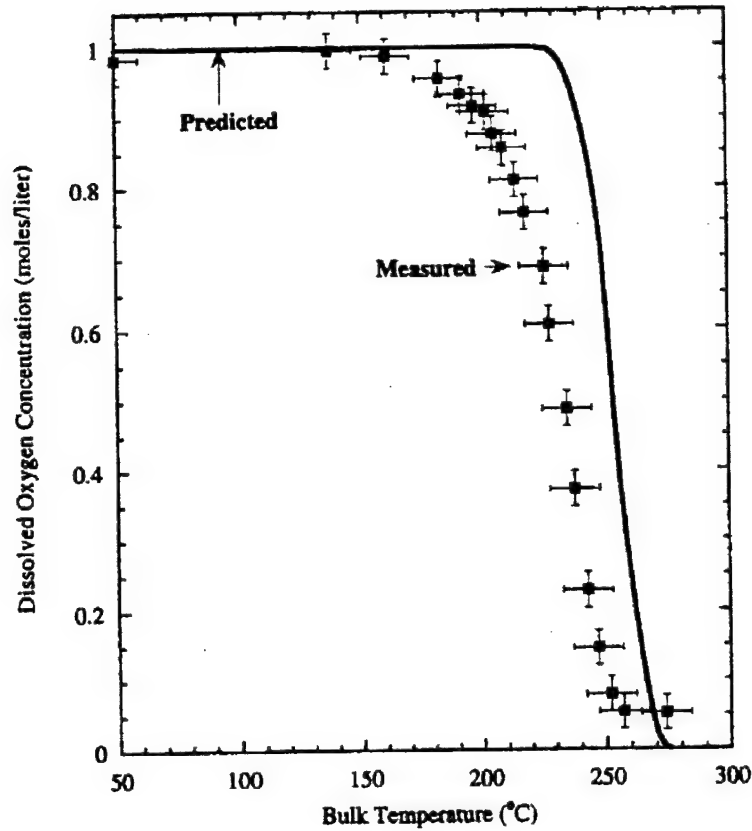


Figure 2: Predicted and measured dissolved O<sub>2</sub> (16mL/min and Jet A) [5]

Katta et al. [7] developed a modified nine-step global chemistry model that improves the accuracy in predicting oxygen consumption, surface deposits, and insoluble particles in the bulk flow. Previous models were incapable of simultaneous prediction of deposition and oxidation rates for blended fuels such as Jet A. His calculations were performed using a CFDC code known as

"foul2d". Katta's work focused only on thermal oxidation with a range of temperatures below the pyrolytic threshold.

## Pyrolytic Research

Since the thermal cracking chemistry of hydrocarbon fuels is not well understood, a detailed CFDC thermal cracking model for pyrolytic conditions is not practical. However, global chemistry modeling can be used as an initial approach. Sheu et al. [8] used a three step global chemical kinetics model to simulate the thermal cracking of Norpar-13 under supercritical and near critical pressure conditions. A cracked product model was incorporated into the CFD code, CFD-ACE™, where the fluid properties of the mixture were calculated using SUPERTRAPP [9]. Predictions were compared with experimental data measured at different flow temperatures and residence times. The simulated temperature and conversion results were in agreement with the experimental data, where conversion is defined in Equation 1. The experimental conversion values are obtained based on the changes of liquid volume before and after the cracking process as described by Edwards and Anderson [15].

$$Conversion = 1 - \frac{Volume(liquid)_{exit}}{Volume(Norpar13)_{inlet}} \quad (1)$$

The experimental portion of this research utilized a vertical tube constructed from Silcosteel passivated tubing. The tube was electrically heated

by passing a high current through the length of the reactor at a pressure of 1000 psia. Sheu's work is particularly relevant in that it incorporates the software to be used in this study, and is applicable for supercritical flow with pyrolytic reactions.

Striebich et al. [2] used a "micro-reactor" in experiments in which the tube dimensions were 0.02 inch ID, and 0.25 cm in length. A residence time of 83.0 seconds was calculated for dodecane flow rates of 10 mL per hour through the tube. The experiments were conducted at a pressure of 500 psi and a temperature range of 593-704°C where pyrolysis becomes dominant. The results of these experiments showed little deposit formation due to the small flow rates. This reactor has advantages such as small reactant volume, good control of temperature and pressure, and the ability to obtain information quickly over a wide range of conditions. This work set the stage for the current study; the experimental setup and data collection is the same except for reactor length. In this work, Striebich did not confirm his assumption of uniform heating inside the reactor chamber or test his assumption of the temperature profile along the reactor. The wall temperature profile is measured in the present study, in order to properly construct a computational model.

Thermal decomposition of n-decane ( $C_{10}H_{22}$ ) was studied by Yu and Eser [16], [17] under near critical and supercritical conditions. The thermal reaction experiments were carried out in a Pyrex glass tube reactor with a strain point of 520°C. It was found that the thermal decomposition of n-decane under supercritical conditions could be represented by apparent first-order kinetics, even though the decomposition is not a true first order process. An activation

energy of 60 kcal/mole was reported for the n-decane decomposition, which is in good agreement with literature values [18], [19]. This work is important to the present study because it provides important kinetic parameters that are used to construct the computational model.

In a similar study to the present one, Goel [20], used a MATLAB code to model the pyrolysis of dodecane under high pressure conditions. This one step global chemistry model was validated with experimental data obtained at different flow rates in a 1.2 meter reactor with a 91.5 cm heated zone. The simulations were carried out using batch reactor kinetics similar to those discussed by Yu and Eser [16], [17]. The temperatures and pressures in the flow reactor were approximately 600°C and 700 psi, and the properties for the flow were calculated using SUPERTRAPP [9]. For the conditions examined, the model predictions agreed well with experimental results. The experimental and computational results predicted decreasing outlet bulk temperatures and fuel degradation with increasing flow rates. However, the density in this model was assumed constant throughout the reactor flow. Incorporating a variable density into this and future models would predict a more accurate value of outlet bulk temperature and the amount of fuel degradation.

### **III. Experimental Setup and Procedure**

When simulations and experiments are done accurately, discrepancies between the two can shed light on previously unconsidered phenomena. Numerical simulations can be used alone in an analysis, but simulations and

experiments complement each other. Simulations are often calibrated by experiments, and experiments are often interpreted by simulations [20].

For verifying the results of the CFDC model, experiments were conducted with the System for Thermal Diagnostic Studies (STDS) using decane ( $C_{10}H_{22}$ ) as the fuel. The STDS is a flexible mainframe system for conducting many types of thermal analyses on any organic fluid. It incorporates in-line analytical instrumentation to identify products formed from fuel thermal degradation under various conditions. Researchers have used the STDS and similar systems to conduct gas phase thermal decomposition experiments for a variety of materials including hazardous wastes [11], pesticides [12], model mixtures [13], replacement utility materials [14], and other compounds related to high temperature incineration research.

The Air Force Fuels Laboratory fabricated the Condensed Phase Test Cell (CPTC) as an integral part of the System for Thermal Diagnostic Studies. The thermal reaction compartment (TRC) and an analytical gas chromatograph were modified to analyze the products of the fuel. The CPTC/STDS (Figure 3) can be used to conduct experiments for flowing liquids up to 800°C and pressures up to 1500 psig. A product distribution from the exposure of liquid phase and condensed phase materials is accomplished through high-pressure liquid sampling valves in line with gas chromatography and mass spectrometry. This technique is capable of measuring dissolved fixed gases such as nitrogen and oxygen, cracking gases such as methane and ethane, and thermal reaction products of the parent fuel.



In the STDS configuration for the present research, decane was filtered and passed on to a porous sparger (Figure 4) to remove the oxygen from the decane. A constant delivery pump (0-5 mL/min) was used to provide a constant flow rate to the reactor. The liquid was then pumped to a pressure relief valve and passed through two pulse dampeners. The liquid was pumped through 0.02 inch ID 316 stainless steel tubing and sent to a flowing switch valve (Figure 5) that directs the fuel to the high temperature oven and reactor assembly or allows argon to flow through the reactor assembly (Figure 6). When the decane exited the reactor, it was sent to the GC-MS for analysis or switched to exit the high temperature oven where a liquid sample was taken [2].

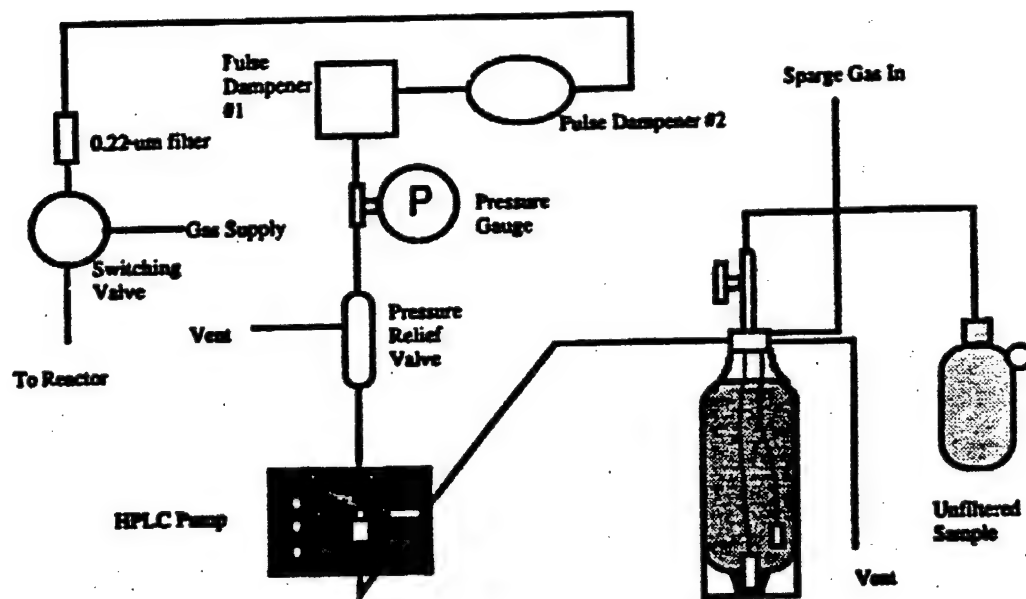
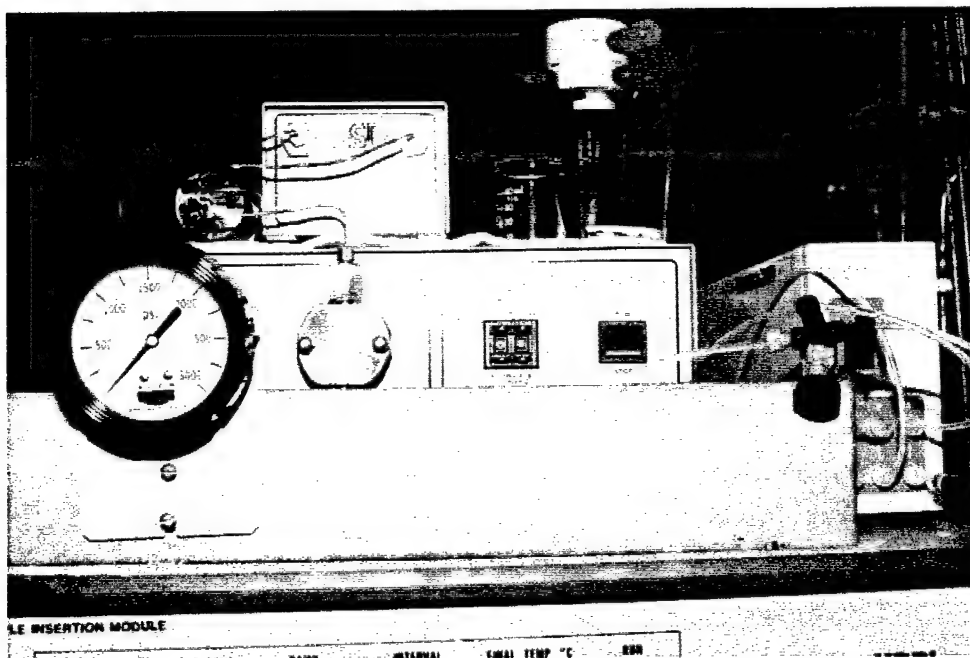
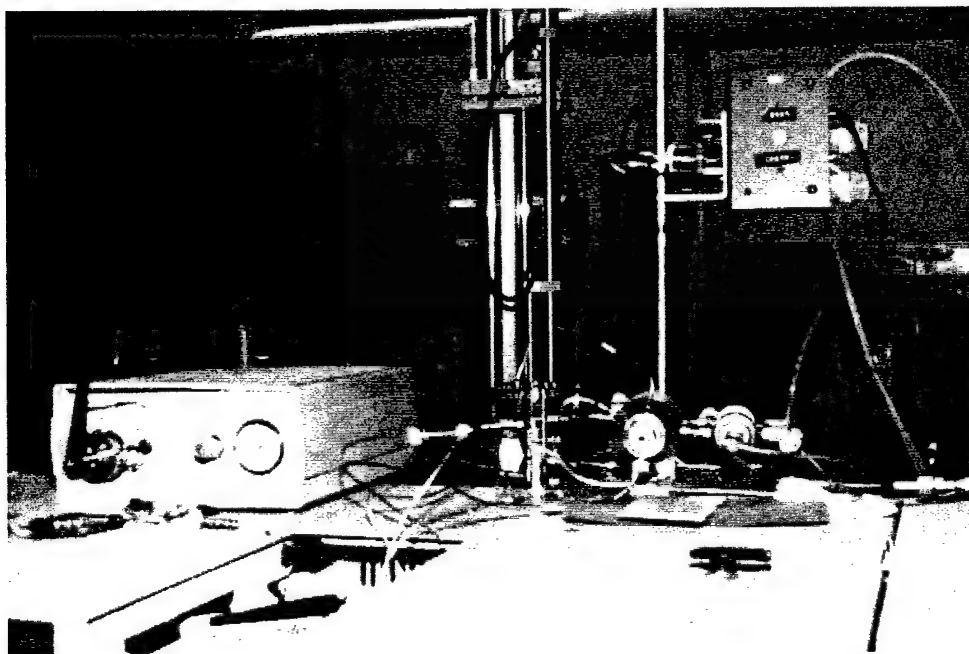


Figure 3: Sample Introduction System for CPTC [2]



**Figure 4: Photo of Sparger, Pump, and Dampener Assembly**



**Figure 5: Photo of Flowing Switch Valve Assembly**

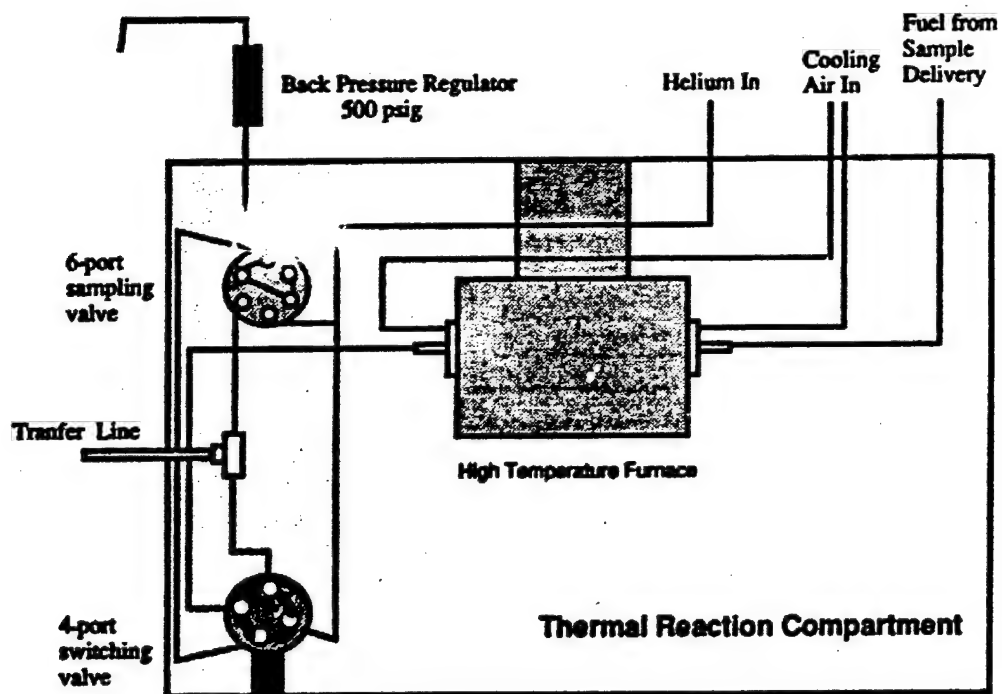
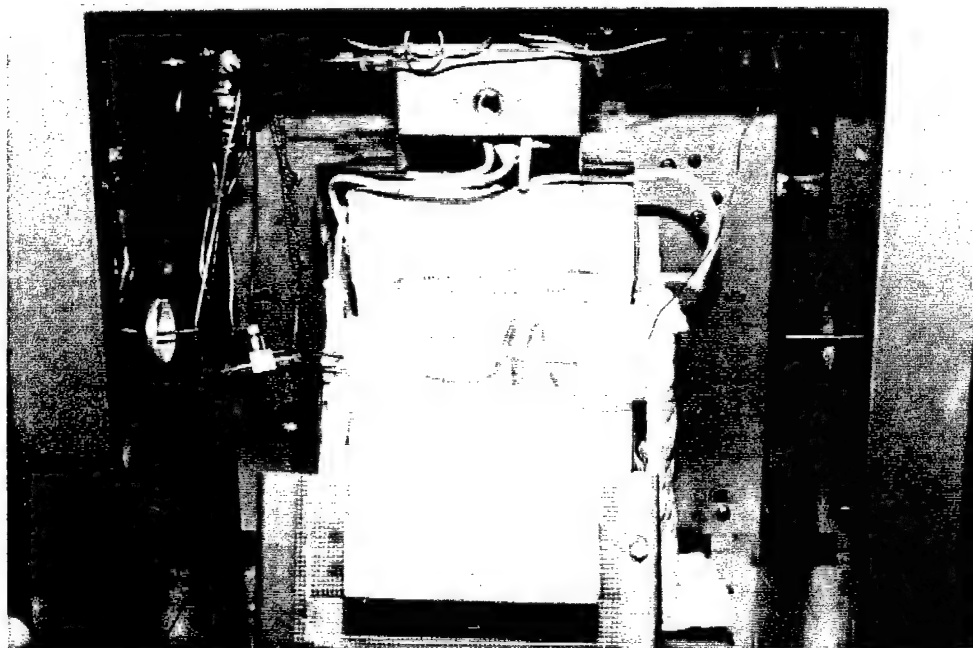


Figure 6: Thermal Reaction Compartment for CPTC [2]

The thermal reaction compartment (Figure 7) consisted of a large oven kept at 200°C with a smaller high temperature furnace inside capable of temperatures reaching 800°C. The high temperature furnace contained a reactor coil 30 cm in length with 0.02 inch ID (Figure 8). Five thermocouples were mounted onto the reactor starting at the entrance to the high temperature furnace with a 2 inch spacing between each thermocouple. These thermocouples recorded the wall temperature profile of the reactor tubing, which are used in the CFDC model of the 30 cm reactor coil. Temperatures inside this reactor ranged

from 200-630°C and maintain a constant pressure of 750 psi. Two flow rates were investigated at 0.5 and 0.7 mL/min.



**Figure 7: Photo of Thermal Reaction Compartment**

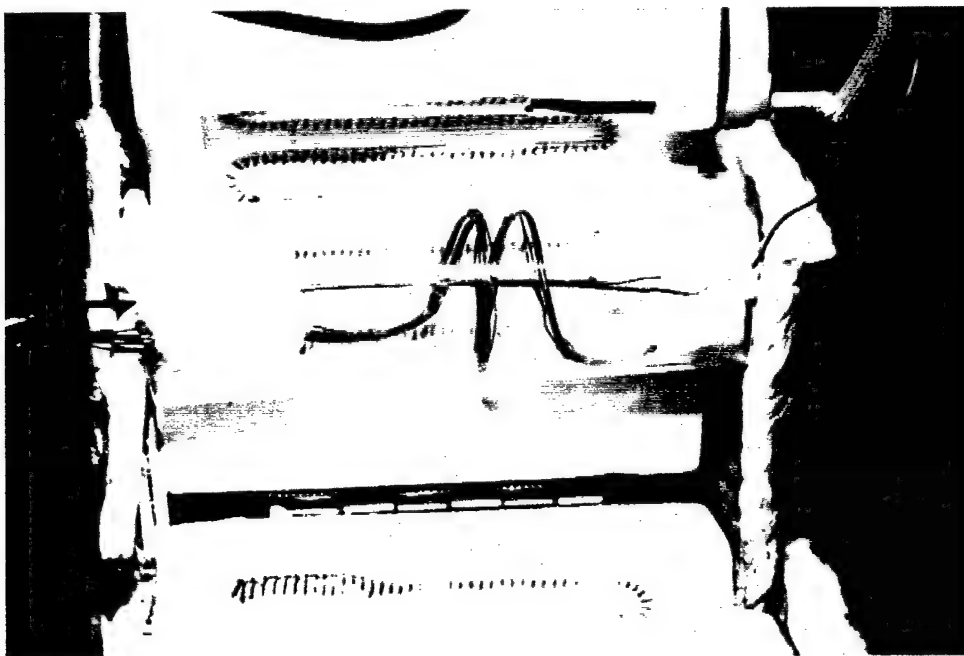


**Figure 8: Photo of 30 cm Reactor Coil Inside High Temp Furnace**

Some critical assumptions have been made when experiments are run using the STDS. The one of most interest to this project is the assumption that the difference between the wall temperature of the reactor and the bulk temperature of the fluid is negligible due to the extremely small diameter tubing and the very low flow rates. Another assumption made in previous work was that the reactor pipe is heated evenly with negligible radiation concentrations inside the reactor. The present study checked and corrected these assumptions.

#### **IV. Computational Model of the Reactor**

The computational model for this project was constructed using the CFD Research Corporation's analysis package including CFD-ACE™, CFD-GUI™, CFD-GEOM™, and CFD-VIEW™. CFD-ACE™ is a structured computational

fluid dynamic flow solver that consists of a preprocessor and analysis code. The preprocessor takes an input file constructed by the user and checks the consistency of the inputs before passing the file on to the analysis code which iteratively solves the proposed problem. Solution values at each cell are written to disk so the results can be extracted for plotting and further analysis. A diagram of the flow solver is shown in Figure 9.

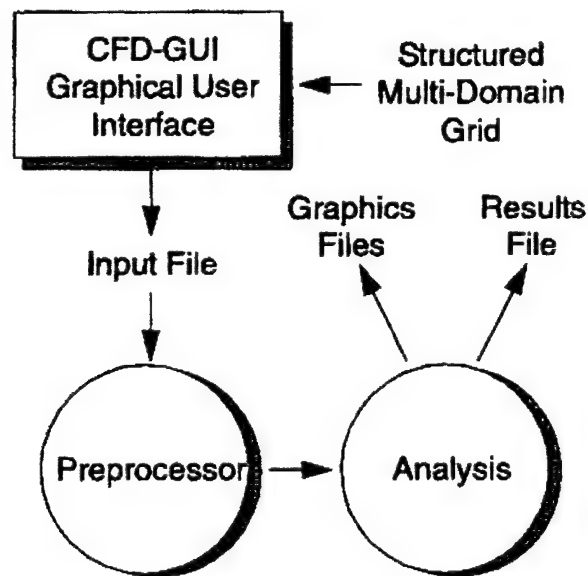


**Figure 9: Schematic Representation of CFD-ACE™ [22]**

Within CFD-ACE™, fluid flows are simulated by numerically solving partial differential equations that govern the transport of flow quantities or flow variables. These variables include mass, momentum, energy, turbulence, mixture fractions, species concentrations, and radiative heat flux. The particular model for this investigation does not utilize turbulence and radiative heat flux as the flow is

assumed laminar ( $Re = 1500$ ) [2] with an experimentally obtained temperature profile used as the wall boundary condition. Radiative effects are also assumed negligible. CFD-ACE™ solves the governing equations in a cylindrical coordinate system for 2-D axisymmetric flow problems like the proposed model. These equations can be found many fluid mechanics text [21] and are not presented here.

The proposed CFD-ACE™ model employs finite-volume methodology with first-order upwind differencing, where the governing equation sets for each variable are solved sequentially and repeatedly until a converged solution is obtained [22]. The overall solution procedure for the model is the SIMPLEC algorithm and is shown in Figure 10. SIMPLEC stands for "Semi-Implicit Method for Pressure-Linked Equations Consistent", and is an enhancement to the well-known SIMPLE algorithm. Van Doormal and Raithby [23] originally proposed SIMPLEC as a method for pressure-correction derived from the continuity equation. This method is inherently iterative and the user determines all the parameters that dictate how many times a procedure is repeated. These parameters are the number of iterations (NITER) and the number of continuity iterations (C\_ITER). For each iteration, the program will calculate a residual for every variable at each control cell. In general, a fifth order of magnitude reduction in the residual is desired before declaring convergence of the variable.



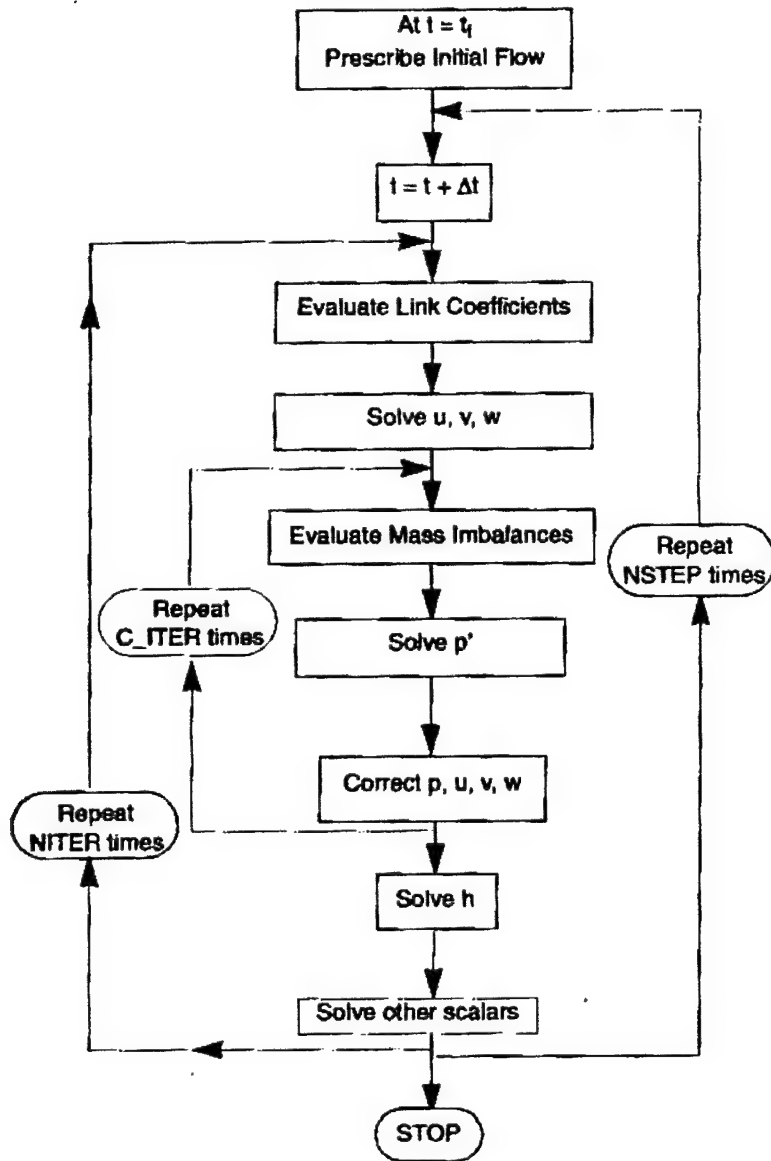


Figure 10: Solution Flowchart for SIMPLEC Algorithm [22]

Ultimately, the computational model needs to not only describe the flow conditions, but also the chemical reactions that accompany the high temperature reactor. Calculation of reactive flow requires the consideration of both stoichiometry and reaction kinetics. Stoichiometry describes the conservation of

mass and elements, while reaction kinetics describes the individual steps that make up a chemically reacting system. There is a distinction between elementary and global reactions. While global reactions are correct in a stoichiometric sense, they do not describe the true path of the reaction, which may be comprised of hundreds of elementary reaction steps. Elementary reactions describe the results due to actual collisions between molecules. The proposed model uses global reactions to model the disappearance of decane. Also, first order kinetics govern the rate of decomposition of decane with a rate constant of the reaction having a temperature dependence expressed in the Arrhenius form:

$$k = A_0 \cdot \exp\left(\frac{-E_a}{RT}\right) \quad (2)$$

The Arrhenius parameters,  $E_a$  and  $A_0$  represent the activation energy and the pre-exponential factor of the reaction, and are determined from batch reactor experiments for decane [16], [17].

The procedure for performing simulations of the reacting decane began with the CFD-ACE™ input file. The CFD-GUI™ (Graphical User Interface) program was not used in this work. The chemistry and boundary conditions used are not compatible with CFD-GUI™, which guides the user through the construction of the input file. Instead, the CFD-ACE™ command language [24] was used to create a custom input file tailored to the specific problem. The input file instructed CFD-ACE™ to use a geometrically modeled grid of the 30 cm high temperature reactor. This 2-D structured grid was constructed with the program

CFD-GEOM™ [25] and has the exact dimensions of the interior of the 0.02 inch ID stainless steel reactor. A small grid study was performed to test the resolution of the computational results. A total of 400 cells were used in the initial grid, and this number was doubled to 800 cells to see if the computations were inaccurate due to the relatively small number of cells. The grid with 800 cells did not improve results and only increased the amount of time needed for computations.

After the grid was read into CFD-ACE™, the input file instructed the program that the problem to be solved is a 2-D axisymmetric, laminar flow, chemically reacting problem with a pressure of 750 psi and an inlet temperature of 200°C. The properties of the flow were calculated with data from SUPERTRAPP [9], and the stoichiometric equations specified in the input file were utilized to calculate the mass fractions of the decomposing decane and product creation along the reactor. The boundary and initial conditions were based on the flow rate and wall temperature profiles from experiment. The kinetic parameters of the reacting flow were taken from Yu and Eser's batch reactor data for decane [16], [17]. CFD-ACE™ terminated the algorithm when an accurate solution had converged. The program CFD-VIEW™ [26] was then used to analyze the computational data. CFD-VIEW™ has the capability of showing the reactor grid (Figure 11) and overlaying the resulting data. Temperature, velocity, pressure, viscosity, and mass fractions of the species can be graphically represented inside the computational grid. Raw computational

data was also saved as ASCII files for analysis in a spreadsheet software program.

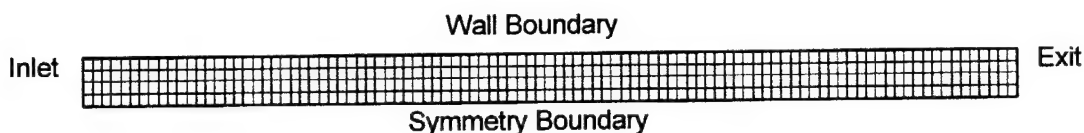


**Figure 11: High Temperature Reactor Grid (Axisymmetric)**

Some assumptions were made for simplification of the model. The flow was assumed to be fully developed, steady state, and laminar with Reynold's numbers less than 2100. The flow is fully developed because it has been flowing in the reactor tubing for over a meter, from the time it enters the sparger to the time it enters the reactor. Striebich [2] calculated Reynolds numbers near 1500 for the STDS which validates the laminar flow assumption. The temperature profile taken at the outer wall of the reactor in experiments was assumed to be the same as the inner wall temperature due to the small reactor tubing and high thermal conductivity of the material, as shown in Appendix C. The decane fuel temperature and concentration was assumed constant and uniform at the inlet. Computational differences between the experimental spiraling reactor and computational straight reactor were assumed negligible. Finally, the kinetic parameters used for the chemistry were assumed to be constant over a temperature range up to 630°C, even though the batch reactions from experiment were only taken up to 460°C. This assumption was made in the absence of additional experimental data for higher temperatures.

## Radiation Effects

Prior to the computational simulations, the experimental data was taken in the STDS as previously described. When the experimental apparatus was completed, the thermocouples mounted on the high temperature reactor were thoroughly tested at temperatures between 200-630°C. Argon was flowed through the reactor, as the high temperature reactor was set at temperatures of 200, 300, and 350°C and the large oven was held constant at 200°C. It was discovered that a temperature spike existed near the center of the reactor most likely due to radiation effects from the radiator coils embedded in the high temperature insulation inside the high temperature furnace.

**Table 2: Temperature Data for Argon Flow Through Reactor**

<i>Thermocouple Along Reactor</i>	<i>Temp. for High Temperature Furnace = 200 °C</i>	<i>Temp. for High Temperature Furnace = 300 °C</i>	<i>Temp. for High Temperature Furnace = 350 °C</i>
1	202°C	293°C	344°C
2	203°C	320°C	380°C
3	204°C	325°C	385°C
4	204°C	319°C	375°C
5	203°C	318°C	375°C

Table 2 shows that as the high temperature furnace was heated above the 200°C oven temperature, the temperature profile deviated from an expected

isothermal profile as shown in Appendix D. The most likely cause of this temperature deviation was radiation effects. These radiation effects were seen because the radiator coils are exposed through their insulation as they heat the high temperature furnace. The stagnant air inside the high temperature furnace also contributed to radiative heat transfer due to minimal absorption, emission, and scatter caused by the air. The view factor concept [27] to examine the radiation exchange between the radiator coils led to an intuition based operational change of the experiment. It is believed that in this case, radiation was the dominant heat transfer mechanism, and this increased radiation concentration raised the temperature near the center of the furnace. To help alleviate this problem, circulation air was introduced into the high temperature furnace to force convection to become the dominant heat transfer mechanism and even the temperature profiles. This circulation air was introduced through a small tube that penetrated the insulation of the high temperature furnace and entered the reactor area as shown in Figure 6.

**Table 3: Temperature Data for Argon Flow with Circulation Air**

<i>Thermocouple Along Reactor</i>	<i>Temp. for High Temperature Furnace = 390 °C</i>	<i>Temp. for High Temperature Furnace = 550 °C</i>	<i>Temp. for High Temperature Furnace = 650 °C</i>
1	392°C	550°C	654°C
2	389°C	540°C	643°C
3	400°C	550°C	649°C
4	389°C	543°C	643°C
5	392°C	542°C	640°C

Table 3 shows that with circulation air inside the high temperature furnace, the radiation effects on the temperature profile were alleviated and allowed for a more isothermal temperature profile inside the reactor. The rise in temperature at the center of the reactor was nearly non-existent compared with the temperature data without circulation air. With the radiation problem reduced, the temperature profiles of the reactor with flowing decane were obtained.

### STDS Temperature Profiles

Temperature data and flow samples were taken for four furnace temperatures and two flow rates for n-decane fuel. The temperatures were 200, 390, 550, and 630°C at 0.5 and 0.7 mL/min. These temperature profiles

**Table 4: Temperature Data for Decane Flow at 0.5 mL/min and 750 psi**

<i>Thermocouple Along Reactor</i>	<i>Temp. for High Temperature Furnace = 200 °C</i>	<i>Temp. for High Temperature Furnace = 390 °C</i>
1	201°C	345°C
2	201°C	368°C
3	201°C	389°C
4	202°C	386°C
5	201°C	387°C

**Table 5: Temperature Data for Decane Flow at 0.5 mL/min and 750 psi**

<i>Thermocouple Along Reactor</i>	<i>Temp. for High Temperature Furnace = 550 °C</i>	<i>Temp. for High Temperature Furnace = 630 °C</i>
1	469°C	550°C
2	517°C	610°C
3	548°C	630°C
4	548°C	629°C
5	549°C	629°C

**Table 6: Temperature Data for Decane Flow at 0.7 mL/min and 750 psi**

<i>Thermocouple Along Reactor</i>	<i>Temp. for High Temperature Furnace = 200 °C</i>	<i>Temp. for High Temperature Furnace = 390 °C</i>
1	201°C	336°C
2	201°C	363°C
3	202°C	390°C
4	201°C	390°C
5	201°C	392°C

**Table 7: Temperature Data for Decane Flow at 0.7 mL/min and 750 psi**

<i>Thermocouple Along Reactor</i>	<i>Temp. for High Temperature Furnace = 550 °C</i>	<i>Temp. for High Temperature Furnace = 630 °C</i>
1	458°C	526°C
2	509°C	592°C
3	549°C	627°C
4	553°C	628°C
5	557°C	629°C



shown in Tables 4-7 are used as boundary conditions for the computational model. Eight separate CFD-ACE™ input files were created using the different experimental temperature profiles as the wall boundary condition of the 30 cm STDS reactor. In the present model, these temperature profiles represent the temperature of inner wall along the reactor for two separate flow rates. Along with the temperature data, off-line and on-line samples were taken for each furnace temperature and flow rate. The samples were analyzed to determine their chemical composition so the amount of decane decomposition could be found. These experimental data points were used for comparison with the computational model.

## **V. Results and Discussion**

### **STDS Reactor Simulations**

With the wall boundary condition set as the various temperature profiles that were previously acquired, simulations of the flowing decane reactor were performed. The inlet flow was set according to the two flow rates used in the experiment, and simulations were run for each temperature profile and flow rate.

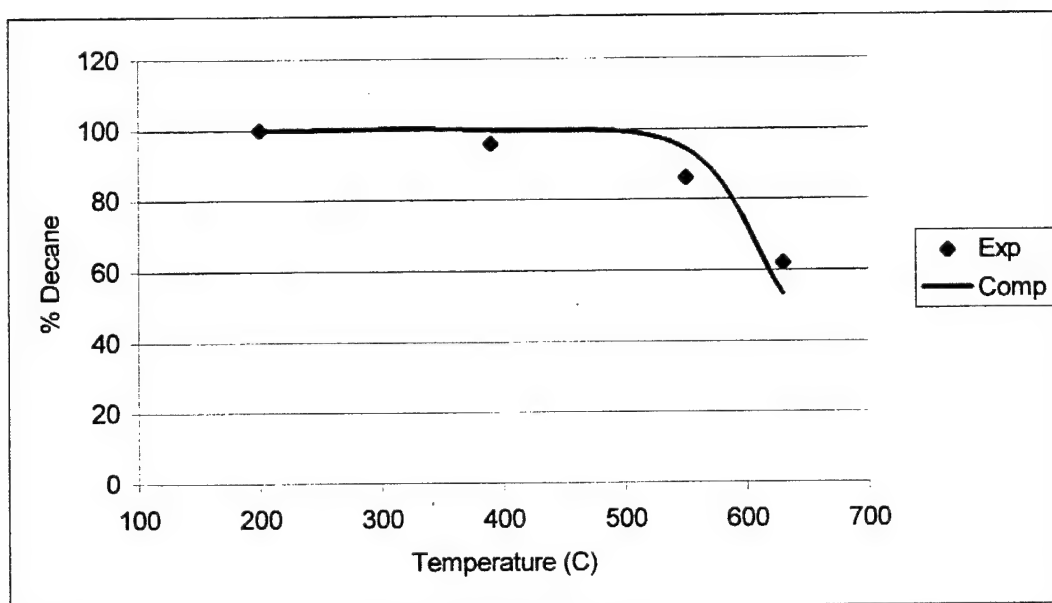


**Figure 12: Decane Decomposition at 0.5 mL/min**

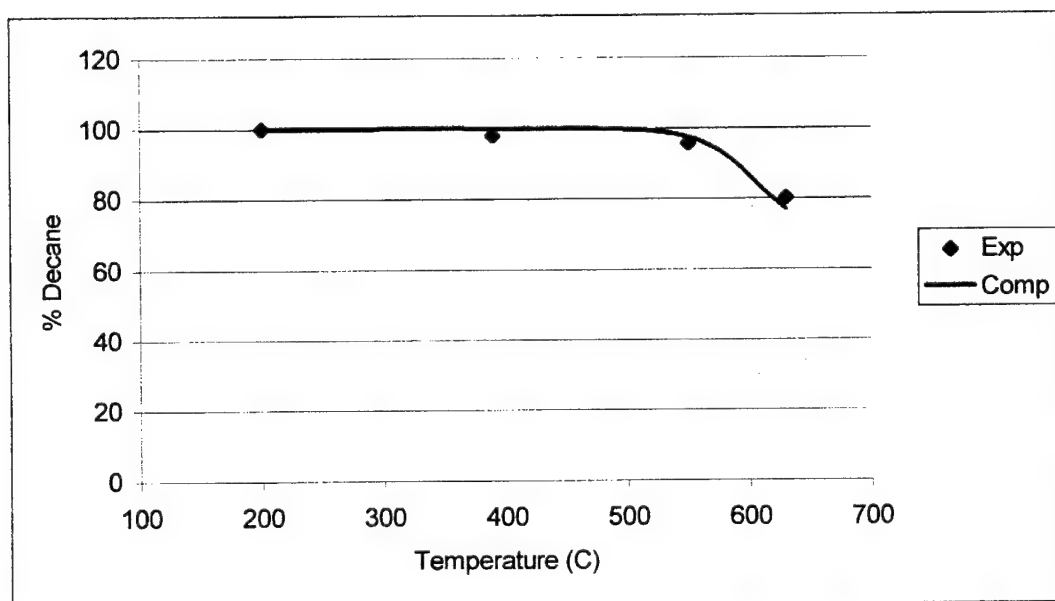


**Figure 13: Decane Decomposition at 0.7 mL/min**

Figures 12 and 13 show the decomposition of decane for both flow rates. For these two plots, the comparison is made between the experimentally measured and the simulated calculation for the decane decomposition at the exit of the reactor. The temperatures shown are the reactor exit temperatures. The simulated calculation is based on global chemistry where decane is assumed to go directly to products based on batch reaction data for activation energy and pre-exponential factor.



Equation 3 shows the simple one step global reaction used for the simulations. This study is only concerned with the decomposition of decane so the product distribution is not analyzed. The activation energy used for these simulations was 60 kcal/mole and a pre-exponential factor of  $6 \times 10^8 \text{ sec}^{-1}$  was found to calibrate this CFDC model. Calibration in this sense refers to "tuning" the appropriate pre-exponential factor so the computational results match the trend in the experimental data. In this model, the "tuning" point was 60% unreacted decane at a furnace temperature of 630°C for the 0.5 mL/min flow rate. This pre-exponential factor was used along with the activation energy to compute the data shown in Figures 12 and 13. Decane decomposition is a very complex reaction with multiple reaction steps and stoichiometries, however this simple global approximation appears to do a good job of matching the experimental trends in the data.

In addition to revealing a close match between the trends in the computational and experimental data, Figures 12 and 13 also match physical intuition. For a 0.5 mL/min flow rate, the decane doesn't begin to crack and degrade until the wall temperature of the reactor reaches approximately 500°C. The decane begins to degrade near 525°C for the 0.7 mL/min flow rate. This was expected due to the higher flow rate and smaller residence time for the faster flow. The decane has less time in the reactor and doesn't degrade as fast as the slower flow at 0.5 mL/min. It is important to note that 40% of the decane is decomposed in the 0.5 mL/min flow, and only 20% of the decane is degraded in the 0.7 mL/min flow. Figure 12 shows how the slower flow rate results in a sharper drop in unreacted decane following initial cracking compared with Figure 13. These results show how chemical kinetics and flow rate are the main controlling factors in the simulated reactor. Table 8 shows the parameters for the experimental model that are used in the CFDC model.

**Table 8: Summary of Parameters for High Temperature Flow Reactor**

<i>Parameter</i>	<i>Parameter Value</i>
Tube OD (m)	0.00159
Tube ID (m)	0.000508
Reactor Length (m)	0.3
Pressure (MPa)	5.2 (750 psi)
Inlet Temperature (°C)	200
Maximum Wall Temperature (°C)	630
$A_0$ (sec <sup>-1</sup> )	$6 \times 10^8$
$E_A$ (kcal/mole)	60

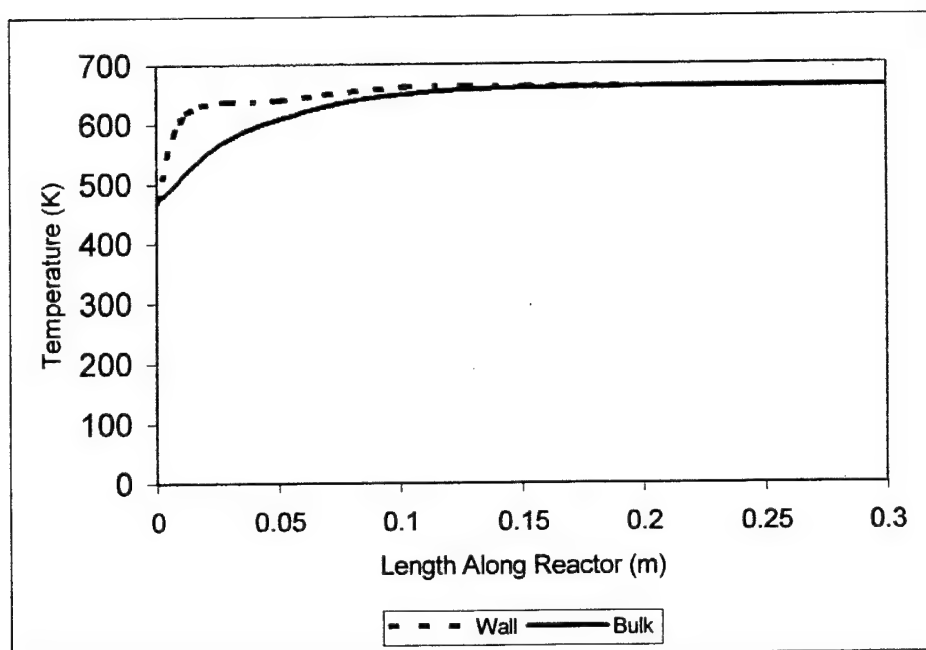


Figure 14: Wall and Bulk Temperature Profile for Reactor at 0.5 mL/min and 390°C

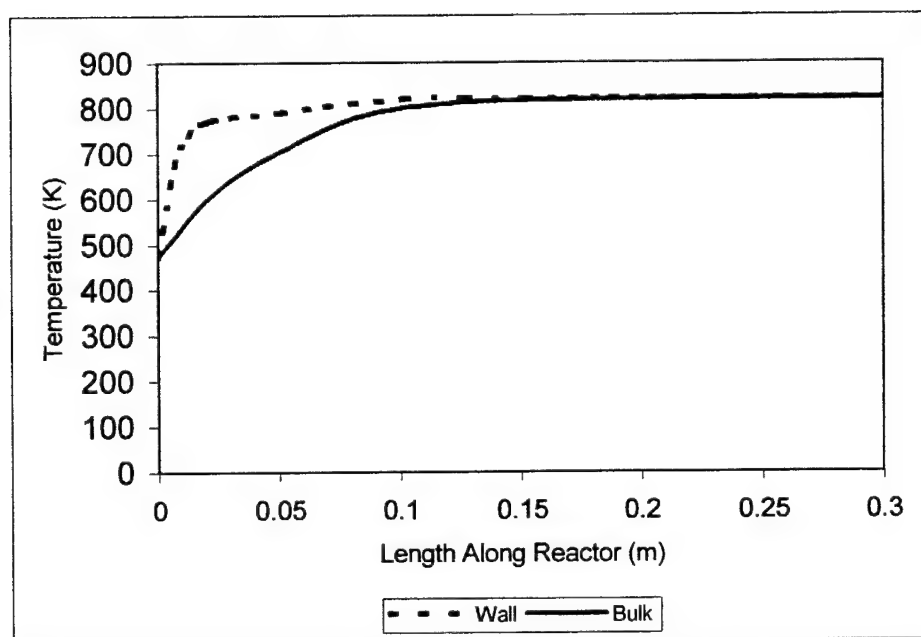


Figure 15: Wall and Bulk Temperature Profile for Reactor at 0.5 mL/min and 550°C

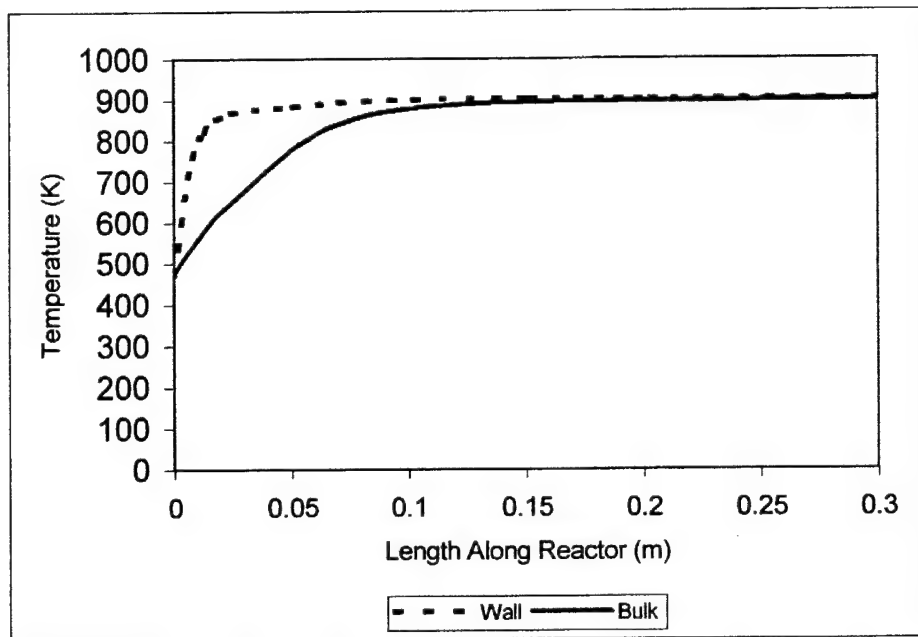


Figure 16: Wall and Bulk Temperature Profile for Reactor at 0.5 mL/min and 630°C

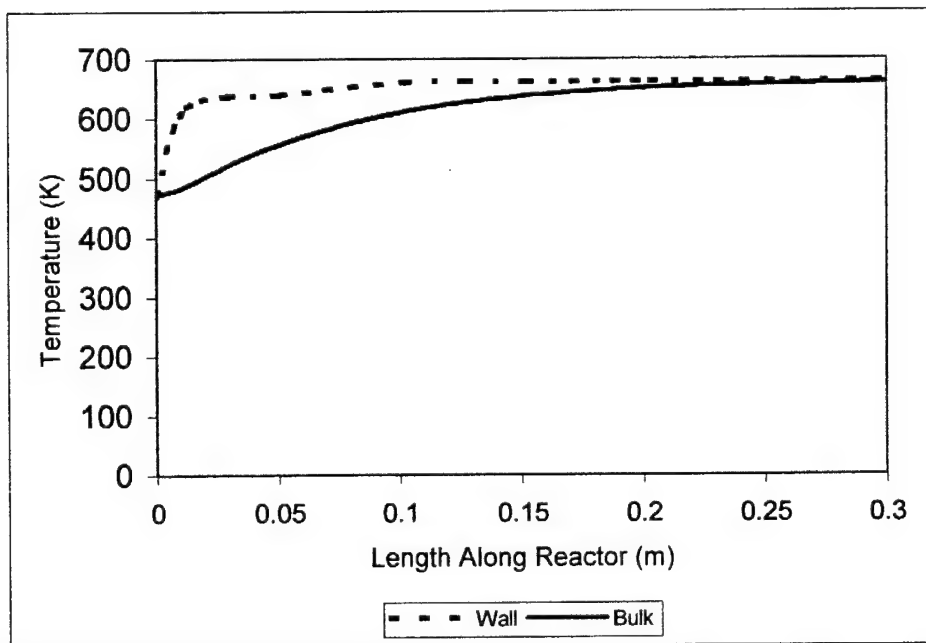
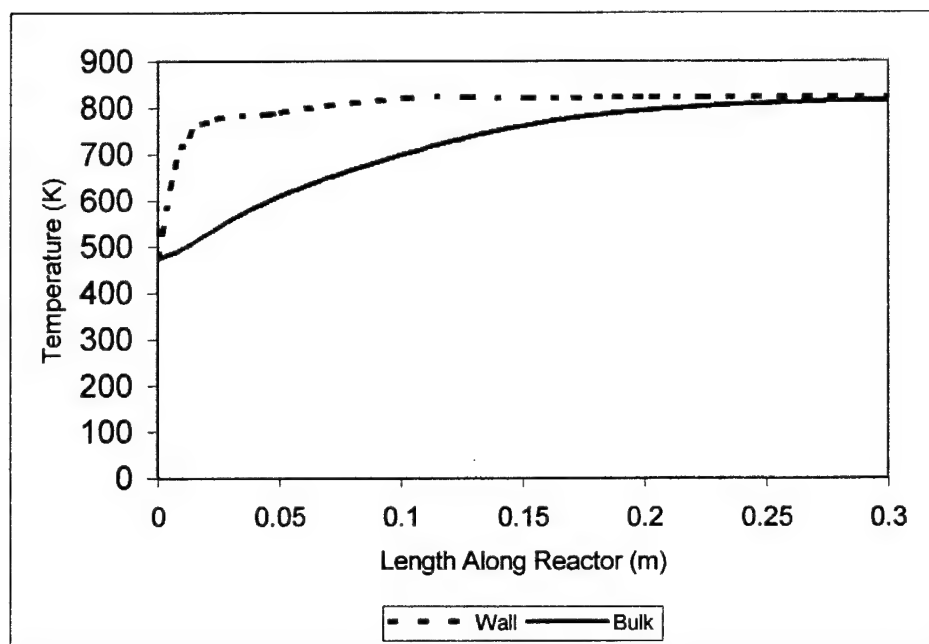
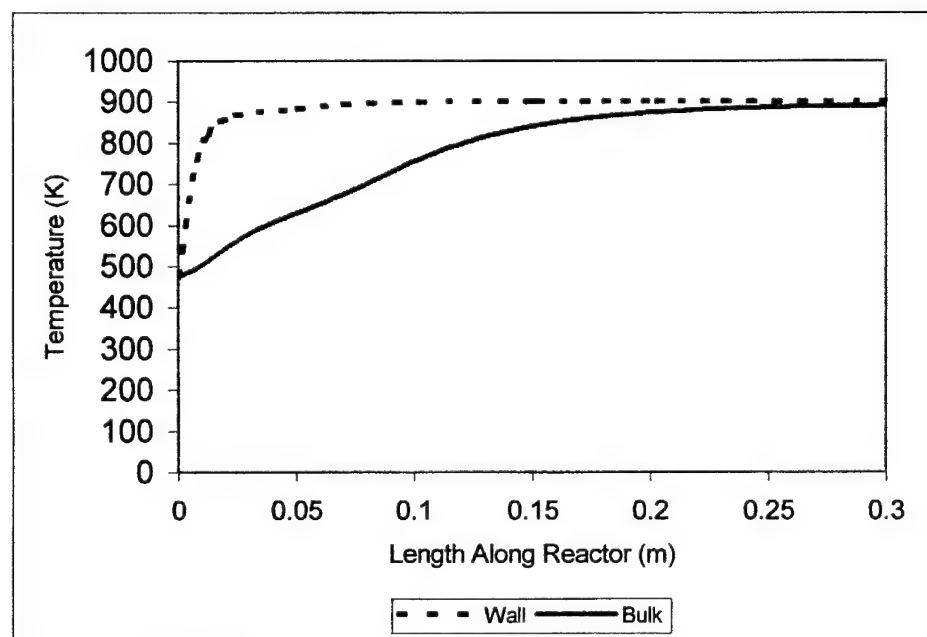


Figure 17: Wall and Bulk Temperature Profile for Reactor at 0.7 mL/min and 390°C



**Figure 18: Wall and Bulk Temperature Profile for Reactor at 0.7 mL/min and 550°C**



**Figure 19: Wall and Bulk Temperature Profile for Reactor at 0.7 mL/min and 630°C**

Figures 14-19 show the computed bulk temperature profiles for each simulation. From these plots, it can be seen that the bulk temperature rises to that of the reactor wall within the first 5 to 10 cm of the reactor for the 0.5 mL/min flow rates. However, the bulk temperature of the 0.7 mL/min flow rates doesn't begin to match the wall temperatures until 15-20 cm down the reactor tubing. As would be expected, it is shown that the start up length of the reactor depends on the flow rate of the decane. Start up length in this case refers to the length of the tube the flow had to travel before the bulk temperature of the decane matched that of the wall. Comparing these temperature profiles with the decane decomposition data describes the overall process. Figures 15 and 16 reveal that the bulk flow reaches temperatures needed for pyrolysis and degradation in the first 5 to 10 cm of the reactor, compared with 15 to 20 cm in Figures 18 and 19 for 0.7 mL/min flow. Because the flow reaches pyrolytic temperatures earlier in the reactor tube at the 0.5 mL/min flow rate, more decane is degraded as the decane moves through the reactor when compared with the faster flow rate. The computed bulk temperature profiles and decane decomposition data complement each other nicely when describing the reacting flow inside the STDS reactor.

### **Larger Reactor Simulation**

To further validate the global chemistry modeling in the present CFDC code, Goel's reactor model [20] was chosen to compare his experimental results for dodecane with a CFDC model for his reactor using the present decane global



chemistry model. Batch reactions [16], [17] have shown that dodecane and decane have similar activation energies, therefore it is reasonable to compare Goel's experimental data with the present global chemistry model. The purpose is to see if the present computational model provides reasonable trends for the decomposition of decane in a larger reactor such as Goel's. Table 8 summarizes the important experimental parameters for Goel's flow reactor that was used in the construction of the CFDC model.

**Table 9: Summary of Parameters for Goel's [20] Dodecane Flow Reactor**

<i>Parameter</i>	<i>Parameter Value</i>
Tube OD (m)	0.00635
Tube ID (m)	0.003175
Reactor Length (m)	0.889
Pressure (MPa)	5.2 (700 psi)
Inlet Temperature (°C)	20
Maximum Wall Temperature (°C)	600

Flow rates of 8, 10, 12, 16, and 20 mL/min were tested experimentally by Goel and are used for the following results of the decane global chemistry model incorporating Goel's reactor. Figure 20 shows that as the flow rate is decreased below 12 mL/min, the computational predictions for decane decomposition don't match the trends in the dodecane experimental data. Since the fuels are different, it is also reasonable to assume that the differences are due to the lack of a more complicated chemistry model. The secondary reactions are ignored in

the present model. As the flow rate is reduced, residence time is greater allowing increased thermal cracking and more decomposition interlaced with multiple secondary reactions.

Another important point is that Goel used a vertical reactor in his experiments. Because of this vertical construction, the effect of gravity can introduce a more complex flow pattern within the reactor. With gravity acting as a body force on the fluid where there are density gradients, a net effect producing a buoyancy force can introduce free convection currents within the flow [27]. The density gradients are due to the temperature gradients within the reactor. The thermal instabilities caused by the warmer, lighter fluid moving upward relative to the cooler, heavier fluid can lead to the transition from a laminar to a turbulent reactor flow. However, Goel calculated a Reynolds number near 800 for the 12 mL/min flow rate, which is well within the laminar regime.

Figure 20 shows the decane decomposition for both the laminar and turbulent flow case, where the turbulent case showed slight improvement in approaching the experimental trends in the data. The turbulent model is two-dimensional and based on a simple  $\kappa$ - $\epsilon$  model [24]. The results suggest the possibility that Goel's reactor might transition to turbulent at lower flow rates where buoyancy forces could affect the reactor flow. A more detailed flow analysis is needed to confirm these suspicions. The main purpose of comparing Goel's experimental data with decane chemistry is to show that the activation energy and pre-exponential factor used in the STDS computational reactions can be successfully applied to a different flow reactor. The data provided in Figure

20 shows that the chemistry model does work in both flow reactors and reveals reasonable trends in decane decomposition.

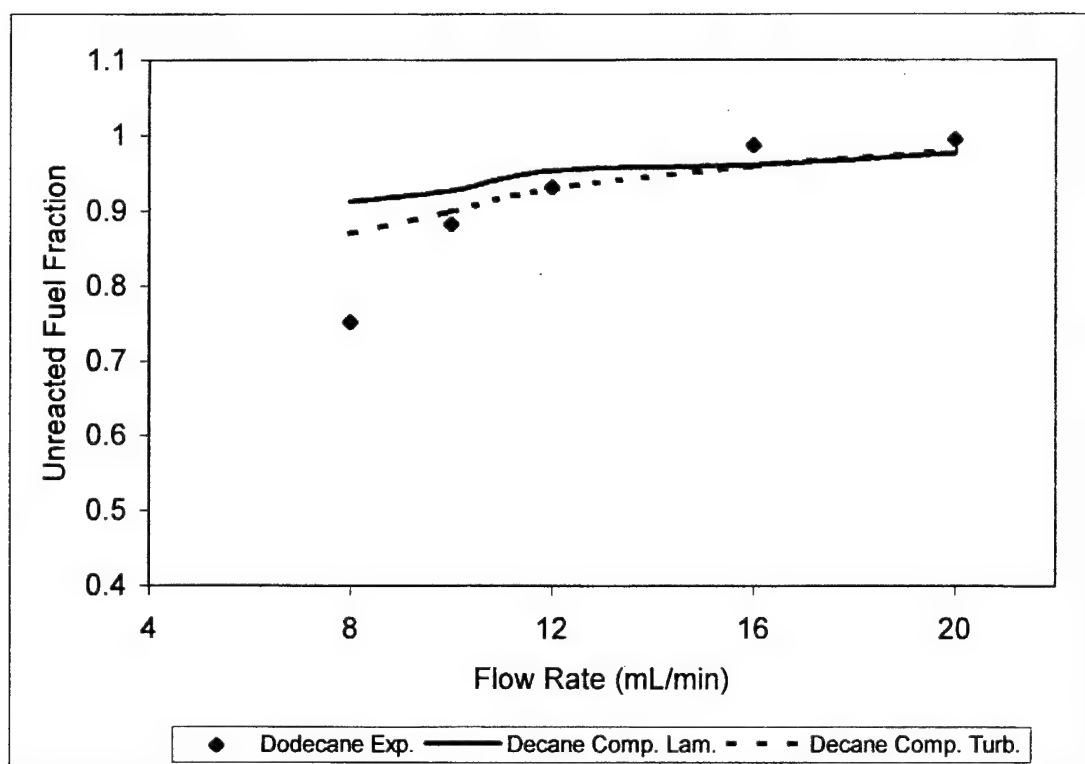


Figure 20: Comparison of Goel's Dodecane Data and Decane CFDC Model

## VI. Summary, Conclusions, and Recommended Future Work

### Summary and Conclusions

This study demonstrates how an off-the-shelf commercial CFD software package can be used to study fuel degradation in a heated flow reactor. A computational model implementing one step global chemistry was used to simulate the pyrolysis of the decane fuel under high pressure and temperature

conditions. This computational model was validated using experimental data obtained from different flow rates where decane fuel was thermally stressed. For the conditions examined from the STDS flow, the model predictions agree well with the experimental results. Both the experimental and computational results show the same effects on the unreacted fuel fraction and temperature profiles with increasing flow rates. The amount of fuel degradation is found to decrease with increasing fuel flow rates.

Under the flow conditions from Goel's reactor, the model predictions differ at lower flow rates because of the possibility of a turbulent transition. However, the global chemistry used in the STDS simulations does reveal reasonable trends in Goel's reactor simulations and suggests that the present model can be used as an important tool in examining various flow reactor geometries. The computational model also serves to study the effects of various physical and experimental parameters on fuel degradation. This computational model can be used to complement experimental results and aid in evaluating how various fuels perform in a heated flow environment. This type of computational modeling with an off the shelf CFDC code also decreases the software development time needed to compare experimental and computational data for air and space vehicle fuel studies.

### **Recommended Future Work**

Considering the complexity of the chemical reactions in the STDS flow reactor, there is a need to add more complex reactions to the chemistry model

within the computational reactor model. A three step or higher global reaction model to simulate the decane decomposition would provide a more accurate description of the chemical reactions, where both the degradation of the fuel and the creation of the products can be studied. More chemistry research is needed to provide the activation energy and pre-exponential factor estimates needed to create such a model.

For reactor flow geometries larger than the STDS, a more detailed analysis is needed to study how turbulence and buoyancy forces affect the chemically reacting flow. A three-dimensional CFDC model would yield more insight into whether advanced turbulence modeling would increase the accuracy of the computational model. Advanced turbulence modeling might prove to take precedence over advanced chemistry modeling if the accuracy in computational data improved dramatically.

Since the present model only studies pyrolytic effects, there is a need to add thermal oxidation into the computational model. The added utility of both pyrolysis and thermal oxidation in the model would give a more accurate description of the physical and chemical processes for a variety of jet and rocket fuels. Also, the computational model has been validated for decane, but more simulations are needed using a variety of fuels to truly verify the feasibility and accuracy of a computational model using a commercial code such as CFD-ACE™.

## VII. Bibliography

1. Moran, M.J., and Howard N. Shapiro. Fundamentals of Engineering Thermodynamics (Second Edition). New York: John Wiley & Sons, Inc., 1992.
2. Striebich, R.C., and W.A. Rubey. A Condensed Phase Test Cell Assembly for the System for Thermal Diagnostic Studies (STDS). Contract F33615-90-C-2047. University of Dayton Research Institute. August 1992 (AD-A258463).
3. Taylor, William F., "Deposit Formation from Deoxygenated Hydrocarbons", Industrial Engineering and Chemistry Production and Research Development, Vol. 13, No. 2, 1974, p. 133-138.
4. Krazinski, J.L., et al., "A Computational Fluid Dynamics and Chemistry Model for Jet Fuel Thermal Stability", Transactions of the ASME, Journal of Engineering for Gas Turbines and Power, Vol. 114, 1992, p. 104-110.
5. Ervin, J.S. and Williams, T.F., "Global Kinetic Modeling of Aviation Fuel Fouling in Cooled Regions in a Flowing System", Industrial Engineering and Chemistry Research, Vol. 35, No. 11, 1996, p. 4028-4036.
6. Ervin, J.S., and Zabarnick, S., "Computational Fluid Dynamics Simulations of Jet Fuel Oxidation Incorporating Pseudo-Detailed Chemical Kinetics", Energy and Fuels, Vol. 12, No. 2, 1998, p. 344-352.
7. Katta, V.R., and Grant, E.G., "Modeling of Deposition Process in Liquid Fuels", 33rd AIAA/ASME/SAE/ASEE Joint Propulsion Conference, AIAA 97-3040.
8. Sheu, J.C., et al. A Joint Experimental/Computational Study of Endothermic Chemistry in Aviation Fuels. Contract F33615-96-C-2619. CFD Research Corporation. September 1998.
9. Ely, J.F., and Huber, M.L., "NIST Thermophysical Properties of Hydrocarbon Mixtures Database (SUPERTRAPP)", V.1.0 Users Guide, July 1992.
10. Roquemore, et al., "Fouling in Jet Fuels: A New Approach", Preprints-Symposia on the Structure of Jet Fuels II, ACS Division of Petroleum Chemistry, Inc., Vol. 34, p. 841-849.
11. Carnes, R.C., and Dellinger, B., "A Correlation of Emissions from Laboratory and Pilot Scale Thermal Decomposition of and Organic Compound Mixture", Toxicology and Environmental Chemistry, Vol. 14, p. 307.

12. Tirey, D.A., et al., "The Thermal Degradation Characteristics of Environmentally Sensitive Pesticide Products", US-EPA Cooperative Agreement CR-813938-01-0, May 1991
13. Taylor, P.H., et al., "Oxidative Pyrolysis of CH<sub>2</sub>Cl<sub>2</sub>, CHCl<sub>3</sub>, and CCl<sub>4</sub>", International Journal of Chemical Kinetics, Vol. 23, 1991, p 1051
14. Taylor, P.H., et al., "Evaluation of Hazardous Organic Products from the Oxidation and Pyrolysis of Creosote-Treated Wood", 39th Pittsburgh Conference on Analytical Chemistry and Applied Spectroscopy, Feb 1988.
15. Edwards, T., and Anderson, S.D., "Results of High Temperature JP-7 Cracking Assessment", Reno, NV, 1993, AIAA 93-0806.
16. Yu, J., and Eser, S., "Thermal Decomposition of C<sub>10</sub>-C<sub>14</sub> Normal Alkanes in Near-Critical and Supercritical Regions: Product Distributions and Reaction Mechanisms", Industrial and Engineering Chemistry Research, Vol. 36, 1997, p. 574-584.
17. Yu, J., and Eser, S., "Kinetics of Supercritical-Phase Thermal Decomposition of C<sub>10</sub>-C<sub>14</sub> Normal Alkanes and Their Mixtures", Industrial and Engineering Chemistry Research, Vol. 36, 1997, p. 585-591.
18. Fabuss, B.M., et. al., "Thermal Cracking of Pure Saturated Hydrocarbons", Advanced Petroleum Chemical Refining, Vol. 9, 1964, p. 157-201.
19. Rebeck, C. Pyrolysis: Theory and Industrial Practice. New York: Academic Press, 1983.
20. Goel, P. Numerical Simulation of Jet Fuel Degradation in Flow Reactors. MS Thesis, Pennsylvania State University, August 1999.
21. White, F.M. Viscous Fluid Flow (Second Edition). New York: McGraw Hill, 1991.
22. CFD Research Corporation. CFD-ACE™ Theory Manual. Huntsville: CFD Research Corporation, October 1998.
23. Van Doormal, J.P., and Raithby, G.D., "Enhancements of the SIMPLE Method for Predicting Incompressible Fluid Flows", Numerical Heat Transfer, Vol. 7, 1984, p. 147-163.
24. CFD Research Corporation. CFD-ACE™ Command Language Manual. Huntsville: CFD Research Corporation, October 1998.

25. CFD Research Corporation. CFD-GEOM™ Interactive Geometric Modeling and Grid Generation Software. Huntsville: CFD Research Corporation, October 1998.
26. CFD Research Corporation. CFD-VIEW™ 3-D Computer Graphics and Animation Software. Huntsville: CFD Research Corporation, October 1998.
27. Incropera, F.P., and David P. DeWitt. Fundamentals of Heat and Mass Transfer (Fourth Edition). New York: John Wiley & Sons, Inc., 1996.



## Appendix A

### Sample Input File for STDS Reactor Simulations

The following is a sample input file for CFD-ACE. This input file utilizes the wall boundary condition for the STDS at a temperature of 630°C in the high temperature furnace. The products for the chemical reaction are assumed to be  $C_2H_4$  and  $H_2$ , which tend to be large portions of the products in the batch reactor environment [16]. The products are known to be inaccurate, but an assumption for the stoichiometric equation for the global chemistry has to be made to calculate the decane decomposition.

```
*-----*
*   Sample of Input File Using Real-Fluid Property Capability   *
*-----*
*   SUPERTRAPP for Hydrocarbon Mixture Properties of (T,P;C10H22 *
*-----*
*
*
TITLE ' Study of Decane conversion '
MODEL reactor3e
*-----1-----2-----3-----4-----5-----6-----7-----
PARAMETERS
integer LL = 60 , ML=20
real  XL= 1.0, YL =0.75E-3, dy=0.4E-6, DX=YL/1
real  PSI=6897.1, QBtu=3.1538
real  PREin=750.*PSI, dPRESS=-413*PSI, TEmIn=473., TMIN=473.,TMAX=902.
real  QW=400.E3, QW2=35E3*QBtu,QW3=7.8E3*QBtu
*
real  velin= 56.E-2, UA=velin
real  TKin=0.003*velin*velin, TDin=3.*TKin**1.5/YL
real  R0=0. , R1=YL/2. , R2=YL*2./3., R3=YL*3./4.,R4=YL*8./9.,R5=YL
real  U0=UA*2., U1=UA*1.5, U2=UA*1.111, U3=UA*0.875,U4=UA*0.42,U5=0.
END
*-----*
GEOMETRY
GRID 2D BFC AXISYMMETRIC
USE GRID FROM reactor3.DTF DTF
* Cell Types
END
*-----*
PROBLEM_TYPE
SOLVE FLOW HEAT MIXING REACT
END
```

```

*_____
PROPERTIES
THERMO_DATA from DEC-D.DAT
COMPOSITION 1 C10H22 1.0 C2H4EQ 0.0 H2EQ 0.0
*
* REAL-GAS_properties BY SUPERTRAPP_model EXCST equilibrium PRESS=PREin
REAL-GAS_properties BY SUPERTRAPP PRESS=PREin
*
TABLE_RANGE P      MINVAL=PREin MAXVAL=PREin NPOINT=1
TABLE_RANGE T      MINVAL=473. MAXVAL=902. NPOINT=35
TABLE_RANGE F=C10H22 MINVAL=0. MAXVAL=1. NPOINT=11
BEGIN_SUPERTRAPP MASS FEED
  N-DECANE =C10H22 = 0.   +1.   C10H22
  ETHYLENE =C2H4EQ = 0.98592 -0.98952 C10H22
  HYDROGEN =H2EQ = 0.01408 -0.01408 C10H22
END_SUPERTRAPP MASS FEED
*
END
*_____
MODELS
* TURBULENCE LOW_RE APLUS=26. BPLUS=40. Y++ OFF
*
*
REACTION FINITE_RATE
RSTEP 1 LHS 1.0 C10H22 + 0.0 H2EQ
RSTEP 1 RHS 5.0 C2H4EQ + 1.0 H2EQ
RSTEP 1 CONST APF=0.E0 EF=1.E3 TF=0.
*
* MIX_MODE MULTI_COMP
*
SURFACE_REACTION s1
RSTEP 1 LHS 1.0 C10H22
RSTEP 1 RHS 5.0 C2H4EQ + 1.0 H2EQ
RSTEP 1 CONST APF=4.E8 EF=30.2E3 TF=0.
*
END
*_____
BOUNDARY_CONDITIONS
*
INLET 1 1 1 M
  U=0.04 V=0.0 T=473 P=0.0 C=1
*
EXIT_P L L 1 M
  U=0.0 V=0.0 T=902 P=0.0 C=1
*
SYMM 1 L 1 1
*
WALL 1 L M M NORTH
T=PROF_X REA=s1
T 7 FIT=SPLINE
0.0 0.0127 0.0508 0.102 0.152 0.203 0.300
473 823 883 900 902 902 902
END
*_____

```

```

INITIAL_CONDITIONS
  U=0.04 V=0.0 T=473 P=0.0 C=1
*   RESTART from reactor3e.AUR
END
*
OUTPUT
  PRINTF WALLS
  DTF ON
  DTF_SCALARS STRM T RHO P C10H22 C2H4EQ H2EQ
  RES_PRINT ALL
END
*
SOLUTION_CONTROL
  ALGORITHM SIMPLEC
  SCHEME UPWIND ALL
  ITERATION 1000
  SOLVER CG all
  C_ITERATION 1
  S_ITERATION 50 all
  S_ITERATION 250 pp
  S_ITERATION 150 h
  S_ITERATION 50 F1 F2 F3
  INERTIAL_FACTOR 0.01 h
  INERTIAL_FACTOR 0.1 F1 F2 F3
  RELAX 0.8 RHO P
  RELAX 0.5 T VIS
  MAXVAL 1.0 F1 F2 F3
  MINVAL 0.0 F1 F2 F3
  MINVAL TMIN T
  MAXVAL TMAX T
*
  PDAMP 1.0
END
*
INTERNAL
  MODVDS 0
  INFO 1
END

```

## Appendix B

### Sample Input File for Goel's Reactor Simulations

```
* _____ *
*   Sample of Input File Using Real-Fluid Property Capability   *
* _____ *
*   SUPERTRAPP for Hydrocarbon Mixture Properties of (T,P;C10H22) *
* _____ *
*
*
TITLE ' Study of Decane conversion '
MODEL goel02
*—1—2—3—4—5—6—7—
PARAMETERS
  real PSI=6897.1
  real PREin=700.*PSI, TMIN=293., TMAX=873.
END
* _____
GEOMETRY
  GRID 2D POLAR ORTHOG
  L 200 ; M 8
  xgrid 1  LP1  0. 0.889
  ygrid 1  MP1  0. 0.00159
END
* _____
PROBLEM_TYPE
  SOLVE FLOW HEAT MIXING REACT
END
* _____
PROPERTIES
  THERMO_DATA from DEC-D.DAT
  COMPOSITION 1 C10H22 1.0 C2H4EQ 0.0 H2EQ 0.0
*
  REAL-GAS_properties BY SUPERTRAPP PRESS=PREin
*
  TABLE_RANGE P      MINVAL=PREin MAXVAL=PREin  NPOINT=1
  TABLE_RANGE T      MINVAL=293. MAXVAL=873.  NPOINT=60
  TABLE_RANGE F=C10H22 MINVAL=0. MAXVAL=1.  NPOINT=20
  BEGIN_SUPERTRAPP MASS FEED
    N-DECANE =C10H22 = 0.  +1.  C10H22
    ETHYLENE =C2H4EQ = 0.98592 -0.98592 C10H22
    HYDROGEN =H2EQ  = 0.01408 -0.01408 C10H22
  END_SUPERTRAPP MASS FEED
*
END
* _____
MODELS
*
  REACTION FINITE_RATE
  RSTEP 1 LHS 1.0 C10H22 + 0.0 H2EQ
  RSTEP 1 RHS 5.0 C2H4EQ + 1.0 H2EQ
  RSTEP 1 CONST APF=0.E0 EF=1.E3 TF=0.
```

```

*
* MIX_MODE MULTI_COMP
*
SURFACE_REACTION s1
RSTEP 1 LHS 1.0 C10H22
RSTEP 1 RHS 5.0 C2H4EQ + 1.0 H2EQ
RSTEP 1 CONST APF=6.E8 EF=30.2E3 TF=0.
*
END
*


---


BOUNDARY_CONDITIONS
*
INLET 1 1 1 M
U=0.04 V=0.0 T=293 P=0.0 C=1
*
EXIT_P L L 1 M
U=0.0 V=0.0 T=873 P=0.0 C=1
*
SYMM 1 L 1 1
*
WALL 1 L M M NORTH
T=PROF_X REA=s1
T 7 FIT=SPLINE
0.0 0.2 0.4 0.6 0.8 0.889 0.889
293 503 673 773 839 873 873
END
*


---


INITIAL_CONDITIONS
U=0.04 V=0.0 T=293 P=0.0 C=1
*
RESTART from goel02.AUR
END
*


---


OUTPUT
PRINTF WALLS
DTF ON
DTF_SCALARS STRM T RHO P C10H22 C2H4EQ H2EQ
RES_PRINT ALL
END
*


---


SOLUTION_CONTROL
ALGORITHM SIMPLEC
SCHEME UPWIND ALL
ITERATION 1000
SOLVER CG all
C_ITERATION 1
S_ITERATION 50 all
S_ITERATION 250 pp
S_ITERATION 150 h
S_ITERATION 50 F1 F2 F3
INERTIAL_FACTOR 0.01 h
INERTIAL_FACTOR 0.1 F1 F2 F3
RELAX 0.8 RHO P
RELAX 0.5 T VIS
MAXVAL 1.0 F1 F2 F3

```

MINVAL 0.0 F1 F2 F3  
MINVAL TMIN T  
MAXVAL TMAX T

\*

PDAMP 1.0  
END

\*

---

INTERNAL  
MODVDS 0  
INFO 1  
END

## Appendix C

### Finite Difference Analysis to Study Inner and Outer Reactor Wall

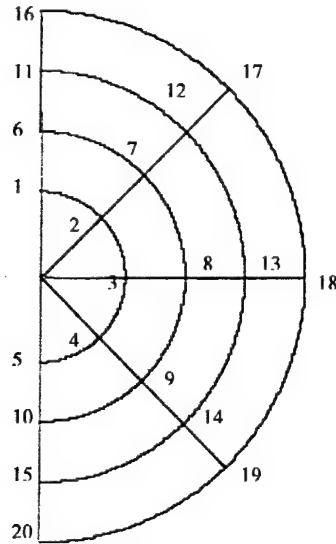


Figure 21: 2D Sketch of the axisymmetric flow reactor

The purpose of this section is to describe the basis for the assumption that the inner wall temperature of the reactor tubing can be approximated as the measured outer wall temperature. Figure 21 above shows a half section of the reactor tube that is axisymmetric. Twenty nodes were set up in a finite difference grid format to examine how the outer wall temperatures and the thermal conductivity of the fluid affect the inner wall temperatures. The  $\Delta r$  and  $\Delta \theta$  for each cell are  $1.8 \times 10^{-4}$  meters and 0.785 radians respectively. A simple example of air flowing through the reactor was examined with a heat transfer coefficient of 288 watts/(m<sup>2</sup> K). This heat transfer coefficient was based on an air

thermal conductivity 0.04 watts/(m K) and a Nusselt number of 3.66 for a laminar flow tube. In the figure above, nodes 1-5 represent the inner wall temperatures and nodes 16-20 represent the outer wall temperatures. To make this study of the reactor more interesting, the outer wall is assumed insulated at nodes 18, 19, and 20 with radiation from the high temperature furnace only heating nodes 16 and 17.

When the temperatures of nodes 16 and 17 are set at 873 K (600°C) and the mean temperature of the air is set as 473 K (200°C), the inner wall temperatures from 3 to 5 are compared to the outer wall temperatures from nodes 18 to 20. Nodes 3-5 range in temperature from 805 to 790 K where nodes 18-20 range from 822 to 798 K. This case represents temperature conditions similar to where flow in the STDS enters the high temperature furnace from the 200°C oven. It is discovered that the inner wall temperatures are within 1-2% of the outer wall temperatures for this largest temperature difference that occurs at the entrance of the high temperature furnace.

For the condition where the mean temperature of the flow is raised to a more realistic temperature of 800 K as would be the case for most of the length of the STDS reactor with flow of 0.5 mL/min, the nodes are examined again for the effect. Nodes 3-5 range from 864 to 858 K, and nodes 18-20 range from 864 to 859 K. The temperatures at the inner and outer walls are a near match. For both extremes in temperature, the inner wall temperatures match the outer wall temperatures in this simplified analysis. This simplified approach also shows



how the heat flows around the reactor tube from the radiation at nodes 16 and 17 to heat the entire reactor uniformly.

#### **Assuming 200°C Fluid Temperature at Reactor Entrance**

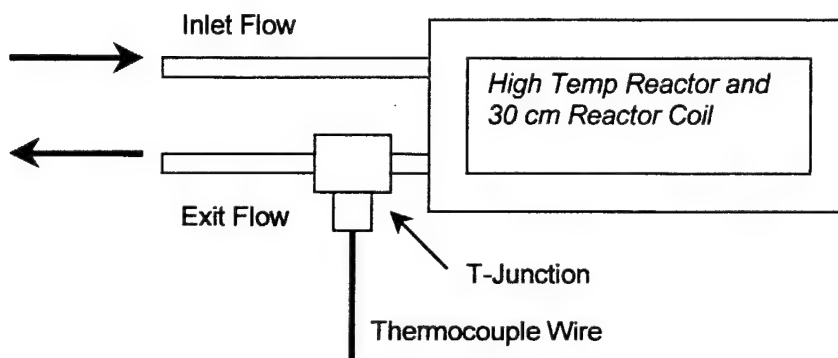


**Figure 22: Sketch of Exit Thermocouple Placement**

During the experimental research, a t-junction and thermocouple were placed on the reactor tube as the flow exited the high temperature reactor as shown in Figure 22. This setup was designed to record a bulk temperature of the decane as it exited the reactor. However, when temperatures inside the high temperature reactor reached 630°C, the exit thermocouple recorded temperatures near 204°C. This thermocouple was placed less than 0.5 centimeters outside the high temperature furnace and the tube and flow had already cooled to the outer oven temperature of 200°C. It was then reasonably assumed that any heat conduction along the tube from the high temperature furnace to the outside reactor tubing along the inlet tubing would be small. This

result then led to the computational model using a reactor wall temperature at the entrance of the high temperature furnace of 200°C.

## Appendix D

### Graphical Representations of Radiation Study Temperature Profiles

The following figures were generated with data taken while examining the radiation effects inside the high temperature reactor. For this study, argon flowed through the reactor tubing. Notice the temperature peak near the center of the furnace without the use of circulation air.

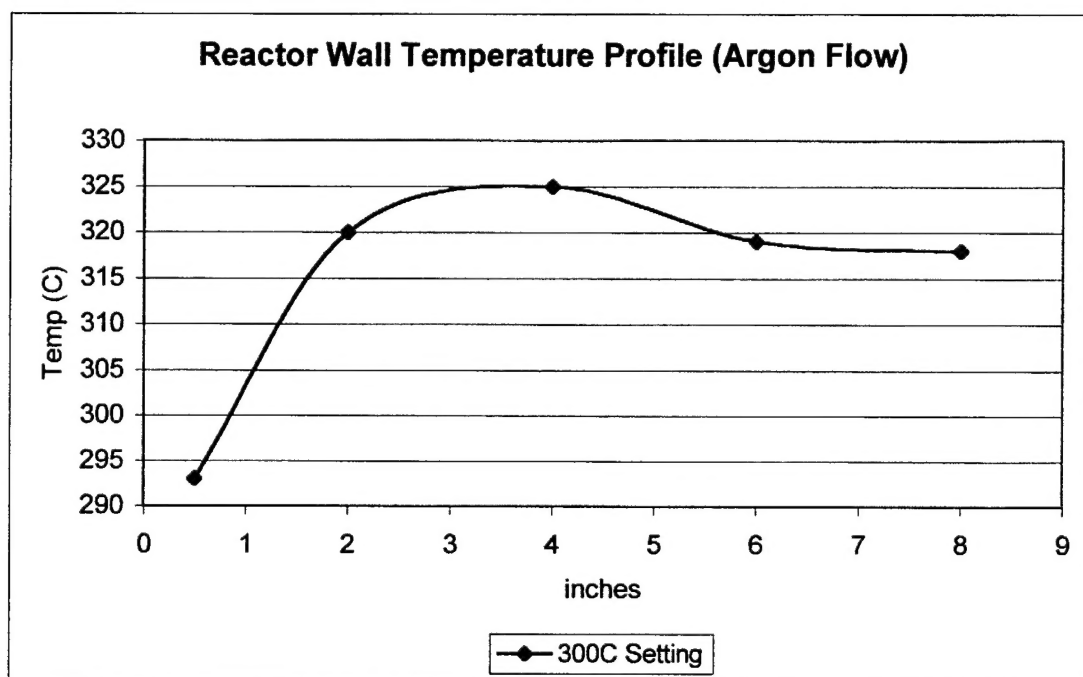


Figure 23: STDS Reactor Profile at High Temp Furnace Setting of 300C

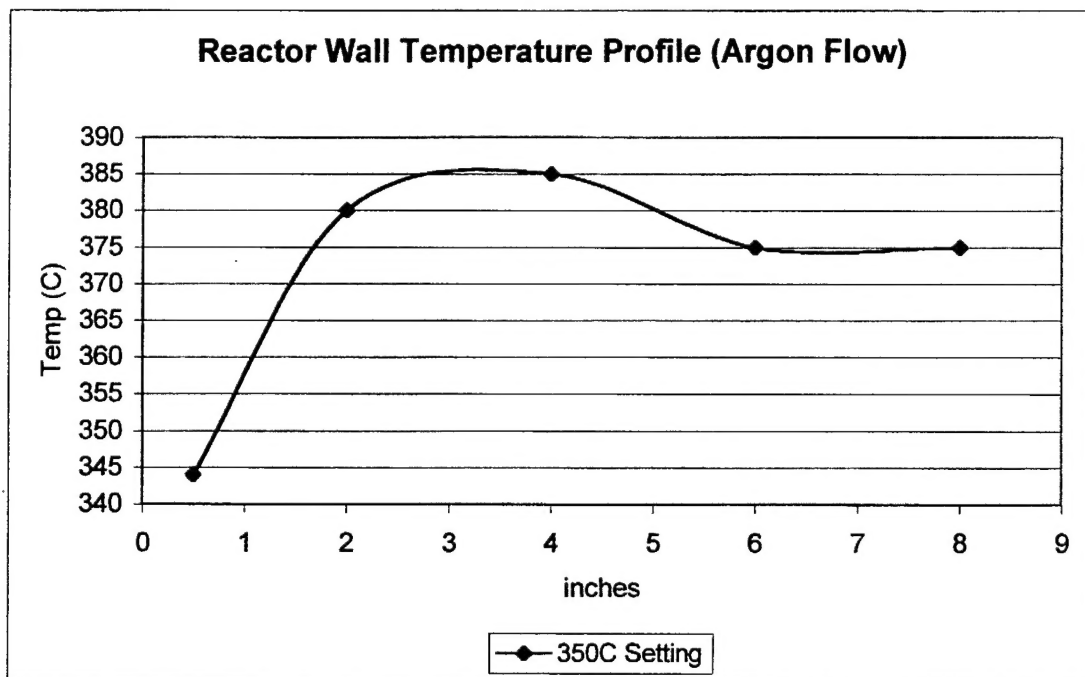


Figure 24: STDS Reactor Profile at High Temp Furnace Setting of 300C

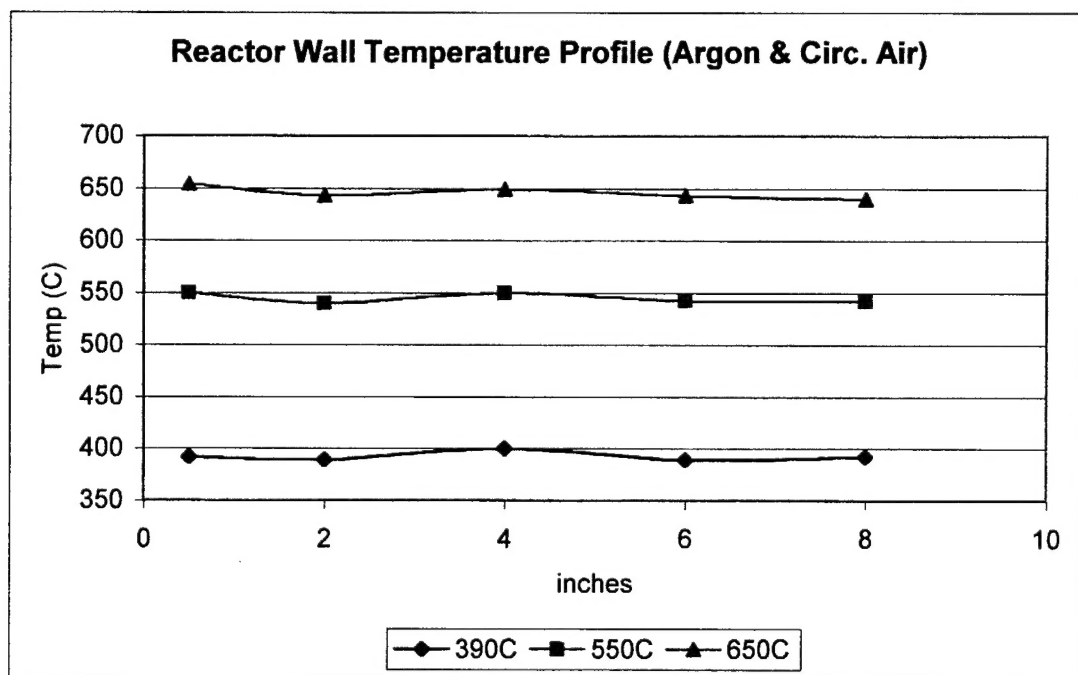


Figure 25: STDS Reactor with Circulation Air for Furnace Temps of 390, 550, and 650C

## **Vita**

Lieutenant Jeff Thornburg was born on 29 July 1973 in Kansas City, MO. At the age of three, his family moved to Benton, IL where he grew up and graduated from Benton High School. Jeff then entered into undergraduate studies at the University of Missouri at Rolla where he graduated with a Bachelor of Science degree in Aerospace Engineering in May 1996. He was commissioned through Air Force ROTC Detachment 442 where he served as cadet wing commander.

Jeff's first assignment was to MacDill Air Force Base, Florida where he served as Sortie Generation Flight Commander. From October 1996 to January 1997, he attended the Aircraft Maintenance Officer Course at Sheppard Air Force Base, Texas, where he was a distinguished graduate. While serving as Sortie Generation Flight Commander, Lieutenant Thornburg deployed to Istres, France from February to April 1997 supporting OPERATION JOINT GUARD as maintenance officer-in-charge for four KC-135R Stratotankers. He also planned, executed, and led a maintenance team for two KC-135R tankers that supported OPERATION BRIGHT STAR in Cairo, Egypt from October to November 1997. In August 1998, Jeff entered the Graduate School of Engineering and Management, Air Force Institute of Technology as a student in the Aeronautical Engineering program. Upon graduation, he will be assigned to the Air Force Research Laboratory at Edwards AFB, CA. Jeff is married to the former Jody Gail Lewis of Keytesville, MO.

REPORT DOCUMENTATION PAGE			Form Approved OMB No. 0704-0188	
Public reporting burden for this collection of information is estimated to average 1 hour per response, including the time for reviewing instructions, searching existing data sources, gathering and maintaining the data needed, and completing and reviewing the collection of information. Send comments regarding this burden estimate or any other aspect of this collection of information, including suggestions for reducing this burden, to Washington Headquarters Services, Directorate for Information Operations and Reports, 1215 Jefferson Davis Highway, Suite 1204, Arlington, VA 22202-4302, and to the Office of Management and Budget, Paperwork Reduction Project (0704-0188), Washington, DC 20503.				
1. AGENCY USE ONLY (Leave blank)	2. REPORT DATE March 2000	3. REPORT TYPE AND DATES COVERED Master's Thesis		
4. TITLE AND SUBTITLE  SIMULATIONS OF FLOWING SUPERCRITICAL N-DECANE		5. FUNDING NUMBERS		
6. AUTHOR(S)  Jeffery T. Thornburg, 1LT, USAF				
7. PERFORMING ORGANIZATION NAME(S) AND ADDRESS(ES)  Air Force Institute of Technology 2750 P Street WPAFB OH 45433-7765		8. PERFORMING ORGANIZATION REPORT NUMBER  AFIT/GAE/ENY/00M-12		
9. SPONSORING/MONITORING AGENCY NAME(S) AND ADDRESS(ES) Dr. Jamie Ervin (937) 252-8878 AFRL/PRSF Bldg 490 Loop Road WPAFB OH 45433-7765		10. SPONSORING/MONITORING AGENCY REPORT NUMBER		
11. SUPPLEMENTARY NOTES  Lt Col Jeffery K. Little, ENY     Jeffery.Little@maxwell.af.mil (334) 953-7848				
12a. DISTRIBUTION AVAILABILITY STATEMENT  Approved for public release; distribution unlimited.			12b. DISTRIBUTION CODE	
13. ABSTRACT (Maximum 200 words) The Air Force is interested in the research of supercritical jet and rocket fuels, as well as the effects of thermally induced fuel degradation. As future flight vehicles travel at ever increasing Mach numbers, greater heat loads will be imposed upon the fuel.  The primary purpose of this study is to develop a computational model for predicting fuel decomposition and bulk fuel temperatures in a simulated heated flow reactor. The System for Thermal Diagnostic Studies (STDS), located in the Air Force Research Laboratory's Fuels Branch, is used to analyze fuels under supercritical temperatures and pressures. Computational simulations of the STDS reactor are performed to better understand the heat transfer, fluid dynamics, and chemistry associated with fuel flow through the STDS reactor. A simplified global chemistry model is incorporated into the computational simulation.  Predictions of the current model are compared to the results of the STDS experiments, which employ flowing n-decane. The proposed computational model is validated using experimental data obtained at different flow rates after thermally stressing the n-decane fuel. The model predictions agree well with the experimentally measured results. The computational model serves as a tool to study how various physical and experimental parameters affect fuel degradation.				
14. SUBJECT TERMS Supercritical Flow, Thermal Degradation, Pyrolysis, Computational Fluid Dynamics, Chemical Reaction, Computational Chemistry			15. NUMBER OF PAGES 69	
			16. PRICE CODE	
17. SECURITY CLASSIFICATION OF REPORT  UNCLASSIFIED	18. SECURITY CLASSIFICATION OF THIS PAGE  UNCLASSIFIED	19. SECURITY CLASSIFICATION OF ABSTRACT  UNCLASSIFIED	20. LIMITATION OF ABSTRACT  UL	